universität wien

MASTERARBEIT / MASTER'S THESIS

Titel der Masterarbeit / Title of the Master's Thesis

Identification of novel regulators of sprouting angiogenesis using haploid ES cells

verfasst von / submitted by

Dana Abdeen

angestrebter akademischer Grad / in partial fulfilment of the requirements for the degree of

Master of Science (MSc)

Wien, 2017 / Vienna 2017

Studienkennzahl lt. Studienblatt / degree programme code as it appears on the student record sheet:	A 066 834
Studienrichtung lt. Studienblatt / degree programme as it appears on the student record sheet:	Masterstudium Molekulare Biologie
Betreut von / Supervisor:	Prof. Dr. Josef M. Penninger

Acknowledgement

Upon finishing my Master's degree, I would like to express my cordial appreciation and gratitude to the people without whom the completion of this work would have been impossible.

Foremost, I could not have imagined having a better scientific and social environment than the remarkable one I found at the Penninger group at IMBA. I am sincerely grateful to my supervisor, Prof. Penninger for giving me the opportunity to be a member of his outstanding lab and be part of a very interesting project that added much to my scientific knowledge and experience. I am also very grateful for the professional feedback and the valuable remarks I received from him in writing this thesis.

I am very thankful as well to my internal supervisor, Reiner Wimmer for all the help, support and guidance that he provided in the course of my master's project.

Besides the outstanding facilities of IMP and IMBA to whom I am sincerely grateful, I would also love to thank all the Penninger lab members for making the working environment so friendly and enjoyable, and for offering help and advice whenever needed.

Special thanks go to my friend Iris Uribesalgo, for offering her help and professional advice at all times and till the very end despite her limited time, and for always encouraging me to overcome any obstacles.

I would also like to express my deep gratitude to my parents, your continuous support and encouragement was always pushing me further. Thank you for believing in me and for always being proud of what I achieve. Without your love, many things would have never worked. Many thanks go as well to my brothers, it has been always nice to feel your love and support. I feel fortunate to have you both by my side. My thanks go also to my friend Maysa for her

continuous support and for encouraging me to always do things the way they should be done. To my friends Renu, Blanka, Goran, Anna, Tanja, Asia, Hagar, Walhan and Nisreen for their friendship and support. I would also like to take this chance to express my deep appreciation, love and longing to the memory of my grandmother whose loss early this year has left an empty spot that no one could ever fill.

Finally, my special thanks and appreciation go to my small family; My friend and life partner Bilal, without your continuous support, help and advice, your cooperation and understanding, it would have never been possible to reach the point of writing these lines. My lovely Bana, thank you for showing me life from another perspective, for being a reason for success, for teaching me how to appreciate time and chances, and for letting me experience how much joy small things could bring to the heart.

Abstract

Blood vessel expansion, remodelling and maturation is a major physiological event that fulfils the embryonic developmental stages and takes part in adult pathophysiology such as ocular diseases or cancer development. The cascade of events that leads to the formation of new blood vessels from already existing ones is termed angiogenesis. Many known and yet poorly understood pathways orchestrate and fine tune the angiogenic process. In this context, genetic loss-of-function screens are a powerful tool to uncover the role of possible players.

Our goal was to find novel angiogenic regulators by designing *in vitro* sprouting models that mimic sprouting angiogenesis *in vivo*. We accordingly chose 32 candidate genes and performed a comparative study comprising wildtype and a mutant gene functions. The comparison was based on elucidating the effect of gene mutations on the sprouting phenotypes in 3D collagen gels. For this purpose, we used conditionally mutagenized haploid murine ES cells. For each obtained candidate gene, we generated sister clones that only differed in carrying the gene of interest either in the mutated or in the wildtype form using Cre-recombination technologies. We also performed competition studies by injecting equal mixtures of wildtype and mutant clones subcutaneously into immunocompromised mice and validated their differential contribution to teratoma vasculature using Fluorescence-activated cell sorting (FACS) analysis and immunohistochemistry.

In summary, our findings revealed that mutagenizing 13 candidate genes resulted in a significant deviation in their sprouting phenotypes compared to their wildtype sisters, exhibiting either a diminished or an enhanced sprouting capacity. Importantly, the sprouting phenotype of our top hits was confirmed in *in vivo* experiments. Thus, we have identified and validated the function of multiple novel angiogenesis genes.

Zusammenfassung

Die Expansion, Remodellierung und Reifung von Blutgefäßen ist ein wichtiges physiologisches Ereignis, das die embryonalen Entwicklungsstadien erfüllt und an der Pathophysiologie der Erwachsenen wie Augenerkrankungen oder Krebsentwicklung beteiligt ist. Die Kaskade von Ereignissen, die zur Bildung neuer Blutgefäße aus bereits bestehenden führt, wird als Angiogenese bezeichnet. Viele bekannte und doch wenig verstandene Signalwege koordinieren und verfeinern den angiogenen Prozess. In diesem Zusammenhang sind genetische Funktionsverlustbildschirme ein wirkungsvolles Werkzeug, um die Rolle möglicher Spieler aufzudecken.

Unser Ziel war es, neue angiogene Regulatoren zu finden, indem wir *in-vitro*-Keimungsmodelle entwickeln, die die Angiogenese von Sprossen *in vivo* nachahmen. Wir haben dementsprechend 32 Kandidatengene ausgewählt und eine vergleichende Studie durchgeführt, die Wildtyp- und Mutanten-Genfunktionen umfasst. Der Vergleich basierte auf der Aufklärung der Auswirkungen von Genmutationen auf die sprießenden Phänotypen in 3D-Kollagengelen. Zu diesem Zweck verwendeten wir bedingt mutagenisierte haploide murine ES-Zellen. Für jedes erhaltene Kandidatengen erzeugten wir Schwesterklone, die sich nur darin unterschieden, das Gen von Interesse entweder in der mutierten oder in der Wildtypform unter Verwendung von Cre-Rekombinationstechnologien zu tragen. Wir führten auch Kompetitionsstudien durch, indem wir gleichartige Mischungen von Wildtyp- und Mutantenklonen subkutan in immunsupprimierte Mäuse injizierten und ihren differentiellen Beitrag zur Teratomvaskulatur mittels Fluoreszenz-aktivierter Zellsortierung (FACS) -Analyse und Immunhistochemie validierten.

Zusammenfassend zeigten unsere Ergebnisse, dass die Mutagenese von 13 Kandidatengenen zu einer signifikanten Abweichung ihrer sprossenden Phänotypen im Vergleich zu ihren Wildtypschwestern führte, die entweder eine verminderte oder eine

erhöhte Keimfähigkeit aufwiesen. Wichtig ist, dass der sprießende Phänotyp unserer Top-Hits in *in-vivo*-Experimenten bestätigt wurde. Daher haben wir die Funktion von mehreren neuartigen Angiogenese-Genen identifiziert und validiert.

Table of Contents

1 Introduction

1.1 Physiology of Vasculature

The continuous circulation of blood throughout the body by a tubular network of blood vessels is crucial for the delivery of oxygen and nutrients to and the disposal of CO_2 and wastes from various body tissues (Carmeliet, Jain 2011a). Therefore, it is not surprising that mammalian cells are located within the 100 -200 µm diffusion limit for oxygen within blood vessels (Carmeliet Peter 2000). The luminal side of blood vessels is lined by a thin layer of cells named endothelial cells (ECs). Known of being highly metabolically active, ECs have well established physiological roles that include the control of vessel diameter, fluid filtration, maintenance of blood fluidity, inflammation, coagulation and the formation of new blood vessels by angiogenesis (Aird 2012), (Griffioen, Thijssen 2014).

1.1.1 Development of Blood Vessels (Vasculogenesis vs. Angiogenesis)

Gastrulation of the embryonic epiblast results in the formation of the three germ layers, endoderm, mesoderm and ectoderm. Cells that constitute the vasculature in murine yolk sac originate from the mesoderm that gives rise to vascular endothelial progenitor cells and hematopoietic progenitor cells (Swift, Weinstein 2009). Following their migration, these precursor cells undergo differentiation and aggregate to form clusters of cells called blood islands. The precursor cells that constitute the clusters at this stage are collectively referred to as hemangioblast (Goldie et al. 2008). Peripheral cells within these clusters, defined as angioblasts, further differentiate and generate the first form of ECs. On the other hand, cells located in the center of these blood islands differentiate into hematopoietic precursors; the future source of blood. (Patel-Hett, D'Amore 2011). The journey of angioblasts transformation into ECs results in the formation of a primitive vessel network called the primary capillary plexus. This *de novo* formation of an

embryonic primary network of blood vessels by the differentiation of EC precursors is referred to as vasculogenesis (Park, Gerecht 2014; Risau 1997).

This process involves multiple steps including differentiation, migration, proliferation and assembly of ECs into the primitive vessel network and the modification of this network is referred to as angiogenic remodeling (Michaelis 2014). This takes place by pruning of vessels accompanied by an increase in their size, a process that forms the branching pattern of a mesh. At this stage, vessels that are merely composed of ECs start to be supported as their walls mature. This involves the incorporation of pericytes and vascular smooth muscle cells (vSMCs) that wrap the blood vessels and secrete proteins along with the ECs extracellular matrix (ECM) to form a basement membrane (George D. Yancopoulos 2000; Carmeliet, Jain 2011a).

Angiogenesis on the other hand is referred to as the formation of new blood vessels from pre-existing ones (Griffioen, Thijssen 2014) and is responsible for the formation of the vast majority of vasculature as part of normal developmental processes in the body such as cardiovascular system development during embryonic life and the repair of tissues in the adult. Angiogenesis also plays a role in multiple diseases that are associated with an increased rate of blood vessel formation such as tumor development, age related macular degeneration (AMD), diabetic retinopathy (DR) or retinal vein occlusions (Adams, Eichmann 2010; Wimmer et al. 2012; Siemerink et al. 2013).

To spark the process of sprouting angiogenesis, ECs need to be activated by pro-angiogenic cues that exist in the surrounding microenvironment such as vascular endothelial growth factor (VEGF) (Griffioen, Thijssen 2014). After activation of ECs, a regulated cascade of events takes place and leads to the formation of new blood vessels. This starts with local degradation of the basement membrane and the extracellular matrix, ECs protrusion and outward migration to form a capillary sprout, followed by proliferation of ECs, lumen formation accompanied by subsequent branching, anastomoses, onset of circulation, and finally the formation of basal lamina, new extracellular matrix and the stabilization of vessels by recruiting pericytes (Griffioen, Thijssen 2014; Smet et al. 2009) (Figure 1.1).

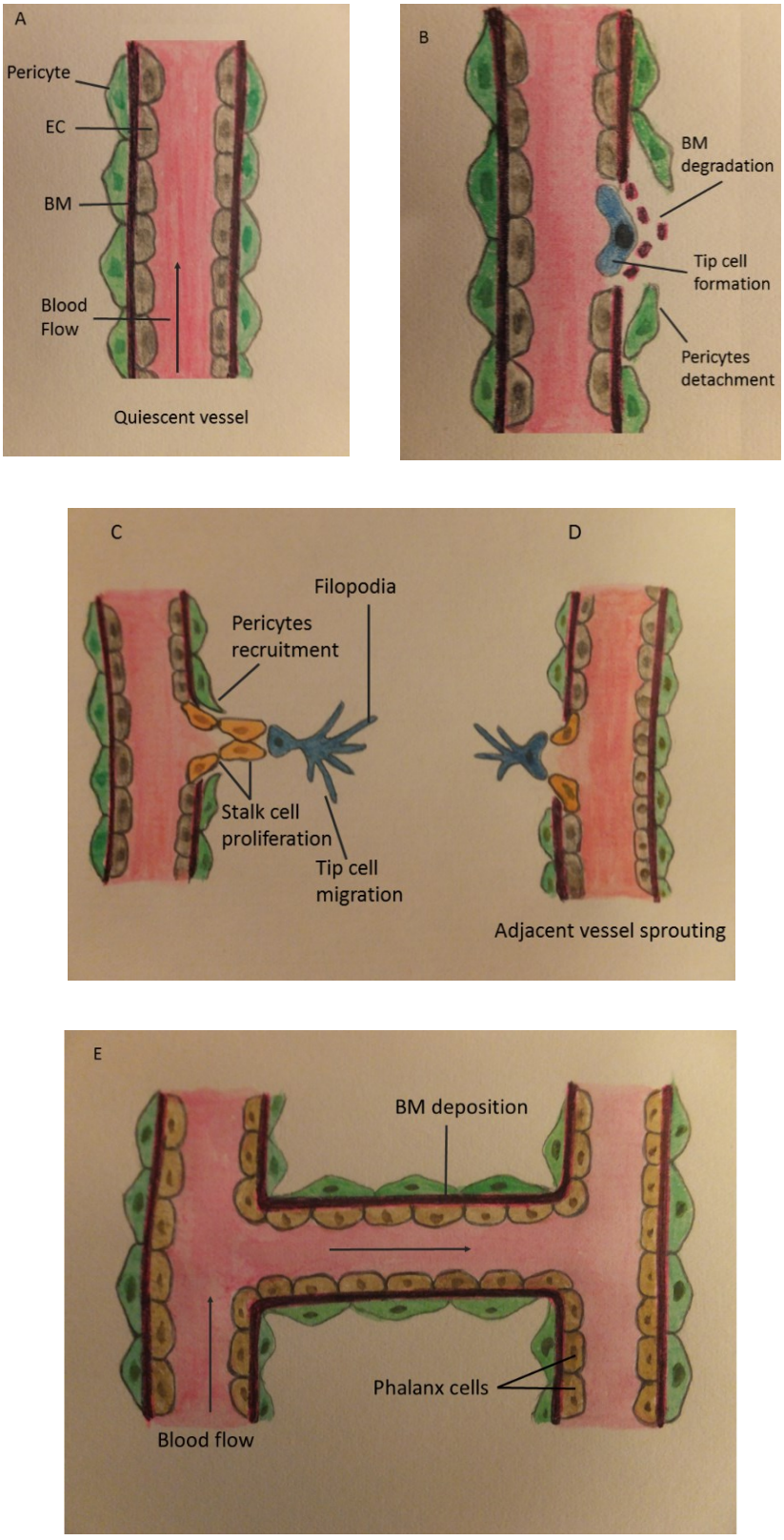

Figure 1.1 Stages of angiogenesis.
A A quiescent vessel before activation by pro-angiogenic cues. EC: Endothelial cells, BM: Basement membrane. **B** Angiogenesis starts upon activation by vascular endothelial growth factor (VEGF) when a

leading tip cell is selected to guide the growing sprout. This is accompanied by local degradation of the basement membrane (BM) which allows the tip cell to protrude and start forming a new branch. **C** The tip cell navigates its way and migrates by means of filopodia formation. Endothelial cells (ECs) following the tip cell are specified into stalk cells whose mission is to elongate and proliferate to form and support the growing sprout. Lumen formation and the consequent blood flow starts in the newly forming vessel. **D** An adjacent growing sprout is meeting the neighbouring growing sprout. **E** Fusion of new blood vessels, blood flow resumption, completion of a new basement membrane and stabilization of vessels by pericytes make up the final steps of sprouting angiogenesis. (Own illustration)

In addition to angiogenesis, other mechanisms of vessel formation include the splitting of a pre-existing vessel leading to the formation of two daughter vessels in a process called intussusception (Carmeliet, Jain 2011a).

1.1.2 Angiogenesis: Tip, stalk and phalanx cells

When vessels that are normally quiescent are subjected to a pro-angiogenic signal, they respond by undergoing sprouting angiogenesis. A hypoxic condition in a nearby tissue triggers the stabilisation and activation of oxygen sensitive transcriptional activators such as hypoxia-inducible factors (HIFs). HIF-induced gene expression in hypoxic cells leads then to the release of angiogenic factors such as VEGF (Carmeliet, Jain 2011a) that stimulates endothelial cell migration and proliferation, and therefore attracts new blood vessels to the hypoxic area. (Park, Gerecht 2014; Chen et al. 2016).

The understanding of the process of new vessel sprouting has become clearer after the identification of the several types of ECs engaged in building up a functional branch: Tip cells, stalk cells and phalanx ECs orchestrate vessel branching each by its specified role (Smet et al. 2009) (Figure 1.1). Tip cells are among the most extensively studied types because of their prominent role in sprouting angiogenesis. Equipped with filopodia protrusions, tip cells are considered the leading cells that are responsible for sensing the pro-angiogenic cues in the microenvironment surrounding them (Smet et al. 2009). The extracellular gradient of VEGF is the main trigger that induces endothelial tip cells to start the process of angiogenesis (Jakobsson et al. 2010). Stalk cells follow the leading tip cell and their role is to proliferate and form a lumen in a way that allows the elongation of the sprout in the direction guided by the tip cell (Smet et al. 2009). On the other hand, and as the original Greek name implies, phalanx cells (named because of their resemblance to the phalanx formation of ancient Greek soldiers) refer to the

cobblestone layer of cells found in the quiescent part of a blood vessel. Phalanx cells are aligned in a smooth monolayer in which cells are connected to each other by tight junctions, shielded by pericytes, and embedded within a thick basement membrane (Figure 1.1). Phalanx cells are involved in basic roles of blood vessels that include sensing and adjusting blood flow as well as tissue perfusion and oxygenation (Smet et al. 2009).

1.1.3 Hallmarks of vessel formation

Sprouting angiogenesis is confined to a limited number of ECs within a branch. The integrity of the pre-existing vascular network is kept intact and well integrated (Siemerink et al. 2013). Angiogenic stimuli lead to the induction of endothelial tip cells whose activity is controlled by the extracellular VEGF gradient (Jakobsson et al. 2010). In order for these endothelial tip cells to start moving towards the attraction cue, they have to be liberated from the surrounding basement membrane that wraps the endothelial tube and that is at the same time shared between the ECs and the mural cells (Potente et al. 2011). This is achieved through proteolytic degradation of the extracellular matrix proteins comprising the basement membrane, and the detachment of smooth muscle cells and pericytes from the vessel wall. Detachment of pericytes takes place in response to Angiopoietin-2 (ANG-2) and the degradation process of the basement membrane is mediated by matrix metalloproteinases (MMPs) expressed by tip cells (Rundhaug 2005; Brudno et al. 2013). Membrane type-1 MMP (MT1-MMP); a MMP rich in tips, was found to be crucial for the invading ability of ECs in adults where the basement membrane is thick and rich in laminin and type IV collagen (Smet et al. 2009). However, during embryonic development where the basement membrane comprises only of a thin layer, loss of MT1-MMP was not found to impede vascular development (Potente et al. 2011; Smet et al. 2009; Carmeliet, Jain 2011a). On the other hand, and while rich in tip cells, it was found that the expression of MMPs in stalk cells is dramatically downregulated during vessel maturation (Smet et al. 2009).

After paving the way for the growing ECs, a single tip cell leads the way out of the existing vessel in a polarized fashion in response to a nearby angiogenic attraction cue. Tip cells

are characterized by having highly dynamic structures that form very shortly after sensing a stimulus; namely filopodia (protrusions of plasma membrane that consist of long parallel filamentous actin) and lamellipodia (a highly branched actin filament mesh near the edge of the cell) (Smet et al. 2009). This allows tip cells to migrate into the extracellular matrix (ECM) to navigate their microenvironment for attractive and repulsive guidance cues (Siemerink et al. 2013; Smet et al. 2009). When tip cells sense an attractive cue, they migrate towards it by means of their filopodia which extend as a result of the polymerization of actin filaments (F-Actin). Moreover, filopodia and lamellipodia of the migrating tip cell induce the forward movement of the whole cell by forming adherent focal contact points that connect their cytoskeleton to the ECM and facilitate the cell movement towards the attraction cue (Smet et al. 2009). After navigating the surrounding and extending the growing vessel towards pro-angiogenic cues, tip cells finally accomplish their mission by connecting to the already-formed nearby vasculature which then establishes a new closed vascular network (Norton, Popel 2016) (Figure1.1). The role of tip cells to probe the environmental cues and lead the vessel growing process is consistent with the finding that these cells generally do not proliferate or form a lumen (Geudens, Gerhardt 2011). Tip cells have also been shown to pave the way for the following stalk cells by producing, along with pericytes, components of the basal lamina which may be used by stalk cells as a template to follow while proliferating (Siemerink et al. 2013).

Trailing behind tips are stalk cells. Contrary to tip cells, stalk cells do not contain filopodia, they undergo proliferation and are responsible for elongating the growing sprout and undergoing anastomoses and lumenogenesis which finally leads to connecting the growing vessel to circulation (Smet et al. 2009). Following stalk cell proliferation, recruitment of pericytes and deposition of a basement membrane provide stabilization and controlled perfusion for the growing sprout (Siemerink et al. 2013). In order for the sprout to elongate, stalk cells also obtain spatial information about the positioning of their neighbours by spreading certain molecules into the extracellular matrix (ECM) around them such as EGFL7 (Carmeliet, Jain 2011a). Once a new vascular branch is formed, endothelial cells following stalk cells differentiate into the non-

proliferating phalanx cells lining the inner layer of the new branch. These cells are covered by pericytes with which they share a basement membrane, and are interconnected by cellular junctions such as VE-cadherin and claudins. (Carmeliet, Jain 2011a; Siemerink et al. 2013).

1.1.4 Tip - Stalk cell determination and interaction

VEGFR and Notch Pathways

Angiogenesis is a highly organized process regulated mainly by a receptor tyrosine kinase (RTK) signal transduction pathway. Members of vascular endothelial growth factors (VEGFs) along with their specified transmembrane tyrosine kinase receptors (VEGFRs) are known to be among the most pivotal regulators of sprouting angiogenesis (Jakobsson et al. 2009). VEGFs include five members; VEGF-A, VEGFB, VEGFC, VEGFD, and PlGF (Placenta growth factor). Among these ligands, VEGF-A (denoted VEGF for simplicity) plays the most prominent role in sprouting angiogenesis and is one of the most extensively studied angiogenic regulators (Blanco, Gerhardt 2013). Research studies led to the discovery of several VEGF-A isoforms denoted by the number of amino acid residues they comprise in humans (VEGF-A-121, VEGF-A-145, VEGF-A-165, and VEGF-A-189). Despite the difference in tissue distribution between these isoforms, they were all shown to bind specifically to VEGFR2 or VEGFR1 (Blanco, Gerhardt 2013; Koch et al. 2011).

Three vascular endothelial growth factor receptors (VEGFRs) were identified in endothelial cells; VEGFR1, VEGFR2, and VEGFR3; also known as FLT1, KDR (or FLK1), and FLT4, respectively (Siemerink et al. 2013). Binding of a VEGF ligand to its specified transmembrane VEGFR causes a conformational change that triggers a homo or hetero-dimerization of the VEGF receptors. This activation leads to trans-phosphorylation of tyrosine residues within the receptor's intracellular domain which in turn enables the activated receptor to recruit many downstream signal transducers that contain SH-2 docking sites to consequently start a sequence of downstream events that include multiple signal transduction pathways that finally lead to the regulation and fine tuning

of angiogenesis depending on ligand-receptor identity (Koch et al. 2011; Blanco, Gerhardt 2013; Volinsky, Kholodenko 2013).

Most notably, the binding of VEGF-A to VEGFR2 was found to be responsible for transducing the most crucial effects of VEGF on ECs. This includes increased permeability followed by EC migration, proliferation and survival (Nilsson et al. 2010; Jakobsson et al. 2009; Hayashi et al. 2013). Mutating either VEGF-A or VEGFR2 in mice results in impaired angiogenesis and lethality. In heterozygous VEGF-A mice, abnormalities in blood vessel formation was detected in the embryo (Carmeliet 1996) and a lethal effect leading to death between days 11 and 12 was reported due to the lack of one allele of VEGF-A (Ferrara 1996). Likewise, disruption of *Vegfr2* gene or generating a mutation in the kinase intracellular domain were both reported to cause death at early developmental stages in mice due to defects in the development of ECs and haematopoietic cells (Shalaby 1995; Sakurai Y 2005).

VEGFR1 which is characterized by a higher binding affinity to VEGF-A, yet by a rather very weak tyrosine kinase activity, was shown to serve as a negative regulator that effectively limits signalling through VEGFR2 by its competitive binding to VEGF-A (Hayashi et al. 2013) (Blanco, Gerhardt 2013). The importance of this negative regulation is evident in the lethal effect reported when *Vegfr1* is knocked out in mice, this leads to death at mid-somite stages due to an overgrowth and abnormal structure of the growing vasculature (Fong 1995). VEGFR3 on the other hand is confined to lymphatic endothelial cells and is usually not expressed in the adult vascular endothelium. However, many studies revealed the re-established role of VEGFR3 in regions of active angiogenesis evident by its expression in the leading edge of the sprout (Smet et al. 2009; Tammela et al. 2008; Barry 2008). In fact, activation of VEGFR3 was proven to be rather critical for sprouting angiogenesis; a study that aimed at using monoclonal antibodies to block VEGFR3 signalling showed an evident diminished sprouting and proliferation capacity of endothelial cells in a sprouting mouse model (Tammela et al. 2008). VEGFR3 was shown to exert its action either by the interaction of VEGFR3 with its ligand VEGF-C or independently from ligand binding (Tammela et al. 2011; Zhang et al. 2010). VEGFR3 and

VEGFR2 were also found to form heterodimers through which they transmit cellular signals thought to be distinct from signals transmitted by receptor homodimers (Smet et al. 2009; Dixelius et al. 2003).

Another signalling system that works side by side with the VEGF-VEGFR system and that is indispensable for proper sprouting angiogenesis and normal vascular development is the Notch signalling pathway. A tight interaction between the VEGF-VEGFR2 pathway on the one hand and Dll4-Notch signalling pathway on the other hand is crucial for EC proliferation and regulation (Benedito et al. 2009). Five transmembrane ligands, Jagged 1, 2 and Dll1, 3 and 4 interact with their Notch transmembrane receptors expressed in the ECs. This interaction results in a conformational change that leads to the cleavage of Notch by γ-secretase and the subsequent release of the Notch intracellular domain (NICD) which exerts its effect in the nucleus by binding to recombining binding protein suppressor of hairless (RBP-J) (Majumder et al. 2016; Boareto et al. 2015). In case of Dll4-Notch signalling, this complex works as a transcription activator of which most targets of which are repressors that dramatically affect and regulate angiogenesis by negative feedback loops (Jakobsson et al. 2009).

Levels of Dll4 and Notch varies between adjacent ECs: High expression of Dll4 was shown in tip cells which leads to more Dll4 signalling from tip cells towards their neighbouring ECs (Jakobsson et al. 2010). Following Dll4 binding, expression of VEGFR2, VEGFR3, and NRP1 in neighbouring cells is dampened leading to their reduced sensitivity to VEGF; this favours the stalk cell phenotype to be adopted in cells adjacent to the leading tip cells which insures that the migratory effect carried out by filopodia extension and the onset of sprouting is strictly confined to the leading edge supported by a proliferating group of stalk cells that trail behind (Smet et al. 2009; Potente et al. 2011). Jagged-1 which has a weaker signalling capacity on the other hand was found to oppose the effect of Dll4-Notch signalling and endorse sprouting by competing with Dll4 (Benedito et al. 2009).

In addition to the two main signalling pathways represented by VEGF-VEGFR and Notch, other ligand-receptor interactions were shown to be crucial for the induction and completion of angiogenesis: For example, Ephrin-B2, a transmembrane ligand that

interacts with EphB receptor tyrosine kinase on adjacent cells plays a role in regulating VEGFR2 internalization which is a critical step required for the activation of the receptor prior to its downstream signalling activity and is important for filopodia extension following VEGF binding (Siemerink et al. 2013; Sawamiphak et al. 2010). Moreover, Ephrin-B2 was also found to play a significant role in controlling VEGFR3 internalization (Wang et al. 2010). Of note, Ephrin-B2 exerts its action in inducing angiogenesis either dependently or independently of the interaction with its Eph receptor (Bochenek et al. 2010; Sawamiphak et al. 2010). Several studies have also highlighted the role of neuropilins (NRPs) in angiogenesis. As co-receptors with short cytoplasmic domains, NRPs were shown to interact with VEGFRs and form complexes that enhance VEGF driven angiogenesis. (Gerhardt 2004; Favier et al. 2006)

Tip – Stalk cell selection

Patterning of the growing sprout into tip and stalk cells is a highly regulated and dynamic process that depends on the interaction and competition between adjacent ECs. (Siemerink et al. 2013; Jakobsson et al. 2010). VEGF-A level that cells are exposed to in their microenvironment is the key factor that decides whether an endothelial cell is going to develop a tip or a stalk cell phenotype. Cells subjected to the highest VEGF-A levels will differentiate into tip cells, extend filopodia, and start probing the nearby microenvironment, whereas cells exposed to lower levels will differentiate into trailing stalk cells that proliferate (Siemerink et al. 2013; Nakayama et al. 2013). This specific sorting of cells needs to be highly regulated in a way that limits the tip cell phenotype in adjacent ECs in order to avoid growth of non-functional over-dense vasculature, and on the other hand, to support the differentiation of other ECs in the growing sprout into proliferating stalk cells that help to support and extend the growing vessel. This tight regulation is controlled by elaborate interacting signalling pathways between neighbouring cells that work through negative and positive intercellular feedback loops; this intercellular signalling system is exemplified in the VEGF-VEGFR-Dll4-Notch-VEGFR feedback loop. (Boareto et al. 2015; Hellström M1 2007).

VEGF-VEGFR-Dll4-Notch-VEGFR intercellular loop

The onset of a new angiogenic sprout begins when an extracellular gradient of VEGF triggers and guides a peripheral endothelial cell in an already existing vessel to differentiate into a tip cell giving rise to a new branch (Potente et al. 2011). VEGF binds to its transmembrane VEGFR2 receptor on ECs. The tyrosine kinase activity of VEGFR2 ultimately leads to an increased expression of membrane bound Notch ligand Dll4 in the tip cell and an interaction between Dll4 and its Notch1 membrane receptor on an adjacent EC. This binding results in multiple proteolytic cleavages of Notch receptor leading finally to liberation of the Notch intracellular domain (NICD) into the cytosol mediated by the ϒ-secretase complex (Mumm, Kopan 2000). Translocation of NICD to the nucleus is followed by its binding to RBP-J. In the absence of Notch signalling, RBP-J works as a transcriptional repressor by interacting with partner co-repressors. However, when NICD enters the nucleus, it binds to RBP-J and triggers the recruitment of a co-activator complex that takes the place of the normally residing co-repressor. This leads to transcription of multiple target genes that ultimately regulate the angiogenic components including some of the Notch ligands themselves such as Dll4 and Jagged1 (Boareto et al. 2015) as well as regulation of VEGF receptors most notably causing down-regulation of VEGRF2 and upregulation of VEGFR1 expression (Miele 2011; Zhou, Hayward 2001; Holderfield et al. 2006; Blanco, Gerhardt 2013). Having this pathway amplified for numerous cycles reduces the sensitivity of these neighbouring stalk ECs to VEGF-A, therefore preventing them from differentiating into more tip cells and rather facilitate their specification into stalk cells. This ensures the presence of only one tip cell leading the growing sprout at a certain point of time followed by proliferating stalk cells supporting the sprout. (Tung et al. 2012; Jakobsson et al. 2010; Venkatraman et al. 2016). Regulation of transcription by Notch also results in downregulation of VEGFR3 and NRP1 in stalk cells (Siemerink et al. 2013). As previously mentioned, VEGFR3 and NRP1 play a role in inducing angiogenesis and their downregulation is therefore consistent with the stalk cell phenotype. Notch signalling in stalk cells leads to an increase of VEGFR1 and its soluble variant sVEGFR1 expression (Blanco, Gerhardt 2013). Binding of VEGF-A to VEGFR1 decoy receptor has an antagonistic effect due to the high

affinity but less sensitivity of VEGFR1 receptor to VEGF-A compared to VEGFR2 which adds more to favouring the stalk cell phenotype in neighbouring ECs (Siemerink et al. 2013; Jakobsson et al. 2009). sVEGFR1 on the other hand contributes to the stability of the stalk cell phenotype by binding to VEGF-A in close proximity to the stalk cells (Harrington et al. 2008) (Figure 1.2).

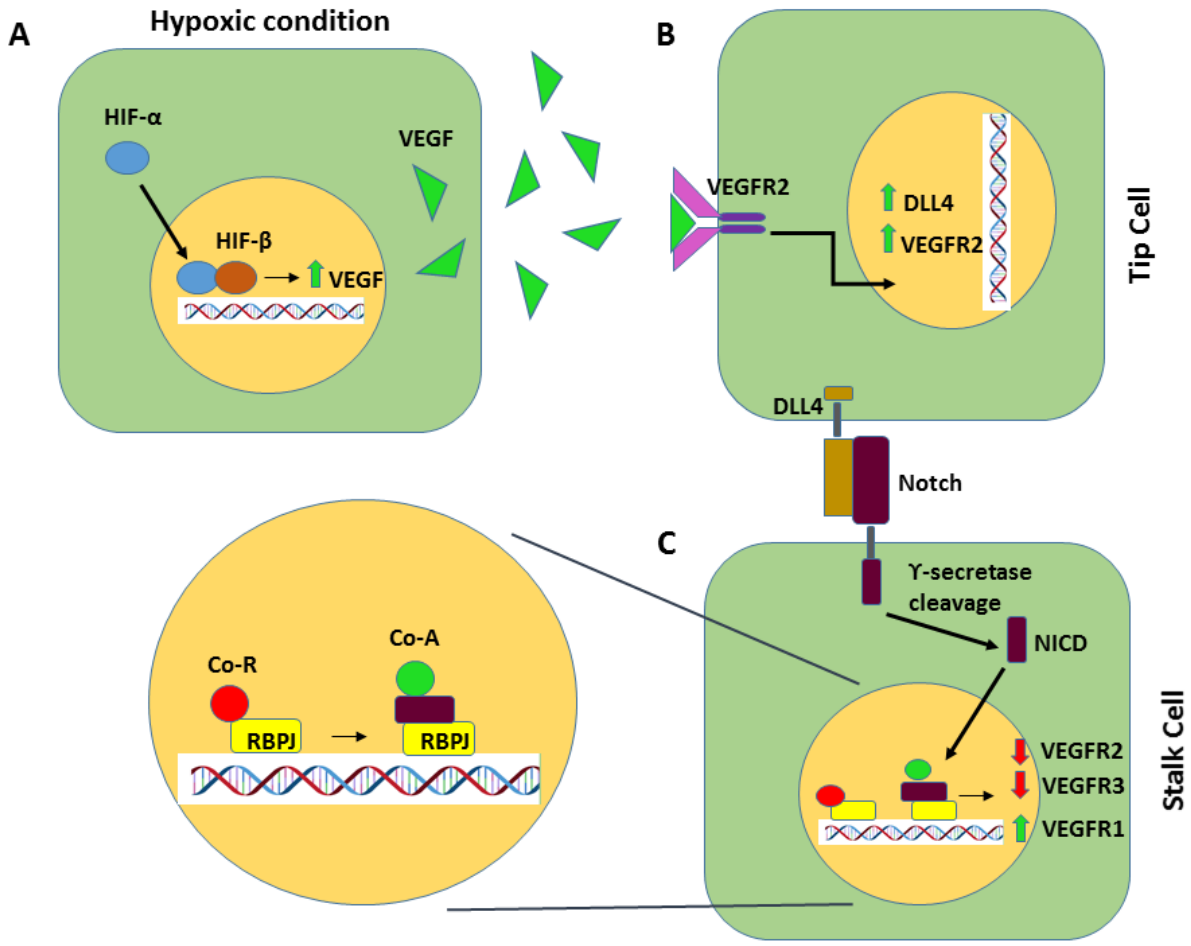

Figure 1.2 Induction of angiogenesis and specification of tip and stalk cells.
A schematic illustration of the main inter- and intra-cellular players involved in angiogenesis. **A** Under hypoxic conditions, hypoxia induced gene expression starts when HIF-α, that is normally subjected to rapid ubiquitination, translocates to the nucleus and heterodimerize with HIF-β subunit resulting in a functional transcription dimer that drives transcription of target genes including *Vegf* by binding to promotors and recruiting co-activator proteins (Goggins et al. 2013). **B** Binding of VEGF to its transmembrane VEGFR2 receptor on a neighbouring EC leads to receptor dimerization and a subsequent conformational change that results into multiple phosphorylation events taking place both on the receptor itself and on downstream signal transducers. Ultimately, these signal transduction events lead to upregulation of both the Notch ligand Dll4, and VEGFR2. This leads to tip cell specification and an

accompanied biological response represented in cell migration towards the ischemic region. **C** Interaction between the activated tip cell and a neighbouring EC occurs via Notch signalling. Notch ligand Dll4 in the tip cell binds to its transmembrane Notch receptor of an adjacent cell. This interaction leads to cleavage of Notch by ϒ-secretase and the liberation of Notch intracellular domain (NICD) into the cytosol following its nuclear translocation where it binds to recombining binding protein suppressor of hairless (RBPJ) and exchanges the previously residing corepressor with an activator complex that initiates transcription of a number of target genes most notably leading to downregulation of both VEGFR2 and VEGFR3 and upregulation of the decoy receptor VEGFR1. The accumulative effect results in rendering the cell less sensitive to VEGF and low in Dll4 which limits its chances to acquire the tip cell phenotype and specifies it as a stalk cell whose role is to proliferate and support the growing sprout. (Own illustration).

The effect of Notch signalling on angiogenesis has been the focus of many studies that revealed its crucial and indispensable role during embryogenesis and development. Targeting Dll1 or Jagged1 were shown to have a lethal effect as mutant mice embryos died early due to severe vascular defects and abnormalities (Xue et al. 1999; Hrabe de Angelis et al. 1997). Intriguingly, Dll4 whose expression during development has been shown to be particularly evident in the arterial endothelium was found to be the only Notch component whose heterozygous deletion in mice results in severe arterial and vascular defects leading to embryonic lethality. This indicates that Dll4 exerts its role in a dosage-dependent manner which makes Dll4 and VEGF the only two angiogenic players whose haplo-insufficiency was reported to be lethal during vascular development (Gale et al. 2004; Blanco, Gerhardt 2013)

Jagged 1 is a Notch ligand characterized by a week signalling activity and is found to be mainly expressed in stalk cells (Blanco, Gerhardt 2013). It has been proposed that Jagged 1 plays a regulatory role for Dll4-Notch signalling. This performs by competing with Dll4 expressed by stalk cells for binding to the Notch receptor present on neighbouring tip cells. By antagonizing the Dll4—Notch signalling pathway between stalk and tip cells, Jagged 1 acts to dampen the Notch activity in tip cells which helps maintain the tip cell phenotype characterized by high expression of VEGFR2 and Dll4 in the leading cell (Benedito et al. 2009; Blanco, Gerhardt 2013).

1.1.5 Tip – Stalk cell dynamics

In a paper published in 2010, Jakobsson and his colleagues used computational modelling to uncover the dynamics of tip and stalk cell selection of ECs during angiogenesis *in vivo* and *in vitro* (Jakobsson et al. 2010). Their findings using live-cell imaging of sprouting angiogenesis showed that tip cell selection is not a stable cell fate but rather a constantly competitive process in which stalk cells alternate and migrate to possess the tip cell phenotype based on the above outlined VEGF-VEGFR-Dll4-Notch-VEGFR feedback loop. The study showed that cells with higher content of VEGFR2 and lower content of VEGFR1 are potentially more likely to possess and keep the tip cell position. VEGFR acts upstream of Notch by regulating Dll4 levels. A computational model using combinations of ECs with different amounts of VEGFR1 and VEGFR2 expression was applied. Predictions concluded from *in silico* visualization comparing wildtype cells and cells heterozygous for *Vegfr2* or *Vegfr1* were in accordance with the genetic mosaic sprouting assays performed *in vitro* and *in vivo*. The *in vitro* model used embryonic stem (ES) cells from mouse (*Mus musculus*). ES cells were cultured in suspension to form embryoid bodies (EBs) that were subsequently cultured in a collagen matrix. 1:1 wildtype cell mixtures from different genetic backgrounds were found to contribute equally to the tip cell position whereas heterozygous cells (*Vegfr2+/egfp*) contributed significantly lesser to the leading tip cells when mixed with wildtype cells in a 1:1 ratio. Importantly, the overall contribution of (*Vegfr2+/egfp*) cells to the growing sprout was not affected by equal mixing with wild type cells as both heterozygous cells and wild type cells contributed almost equally. This favoured the assumption that acquiring the tip cell position is rather a competitive process where the difference in the relative amounts of VEGFR2 and VEGFR1 between cells is one major factor that determines the winning one in the competition process. The role of Dll4-Notch signalling in the tip cell selection process was also highlighted where Notch signalling was abolished in wildtype EBs which resulted in a hypersprouting phenotype both *in vitro* and *in vivo* (Jakobsson et al. 2010).

Recent studies that focused on aspects related to endothelial cell dynamics during formation of new blood vessels have also uncovered some of the secrets that still

hamper the full understanding of the exact mechanisms underlying the process of endothelial cell patterning during vessel sprouting. For example, despite the default tendency of ECs to keep a highly differential Dll4 level that favour heterogeneity between tip and stalk cells during normal angiogenesis (Blanco, Gerhardt 2013), some studies have shown a drift from the normal heterogeneous patterning towards a more synchronized fluctuation of Dll4 levels between contiguous cells under pathological or experimental conditions that expose the active sprouting vessel to high levels of VEGF or to a high cellular Dll4 expression which results in a morphogenic switch of the growing vessel driving it from branching to expansion (Ubezio et al. 2016; Bentley et al. 2009). The expansion of vessels under high VEGF levels was represented by an increase in vessel diameter at the expense of new vessel branching (Ubezio et al. 2016).

1.2 Angiogenesis and disease

Although angiogenesis is crucial for development and regeneration, it is on the other hand key to the progression of many diseases either by failing to fulfil the needs of tissues as a result of inadequate vascular growth evident in myocardial infarction, stroke and neurodegenerative diseases, or when there is an abnormal overgrowth of blood vessels leading to the development of disorders ranging from some eye diseases like age-related macular degeneration (AMD) to tumorigenesis (Carmeliet, Jain 2011a; Potente et al. 2011).

According to the statistics of the World Health Organization (WHO), 7.4 million people died in 2015 because of coronary heart disease which is the leading cause of death worldwide. Therapeutic angiogenesis which aims to re-vascularize ischemic tissues is therefore a very promising field of research that has the potential to benefit millions of people worldwide. Pro-angiogenic therapeutic trials in myocardial ischemia aim to effectively restore perfusion and improve cardiac function in ischemic areas through strategies such as progenitor cell therapy, gene therapy and cell-based gene therapy (Melly et al. 2012). However and despite the extensive body of work in this field, medical trials are still unable to meet the anticipated goals (Carmeliet, Jain 2011a).

In contrast to its promising therapeutic role in vascularizing ischemic tissue, angiogenesis is defined as one of cancer hallmarks due to its critical role in the progression of the disease (Fouad, Aanei 2017). Tumor growth is highly dependent on recruiting surrounding vascular connections for nourishment and waste disposal (Folkman 1971). Therefore, primary solid tumors usually reside near existing blood vessels and metastasis is found to occur in regions of dense vasculature (Lupo et al. 2016). Moreover, tumor cells tend to go through an angiogenic switch under hypoxic and stress conditions causing an increase in the expression of pro-angiogenic factors which in turn leads to increased vessel growth that serves to nourish and aid the tumor cells and boosts its survival (Folkman 1971; Griffioen, Thijssen 2014). However, and like the cancerous tissue itself, the tumor vasculature which is defined as "aberrant angiogenesis" is an inefficient abnormally grown network of blood vessels characterized by being tortuous, fragile, permeable, and structurally and physiologically heterogeneous (Lupo et al. 2016). This fact sparked hopes that targeting main players in the angiogenic process could limit or stop cancer progression and be of therapeutic use (Folkman 1971). Therefore, and despite an overall limited therapeutic progress reported to date, many research and clinical trials have been working on developing tools and strategies meant to abolish the angiogenic activity in tumors.

As stated earlier, VEGF was shown to be the most potent player in driving and regulating angiogenesis (Carmeliet 1996; Ferrara 1996; Yancopoulos et al. 2000), therefore, it was the first choice by which many therapeutic strategies and clinical trials in cancer research (and angiogenic ocular diseases) aimed at targeting (Carmeliet, Jain 2011a). A humanized monoclonal anti-VEGF-A antibody named Bevacizumab (or Avastin) is currently the most clinically effective anti-angiogenic strategy meant to combat a number of solid tumors. The drug was approved by the United States Food and Drug Administration in 2004 (Olsson et al. 2006). However, hopes of treating cancer with VEGF inhibitors were encountered by only a limited success due to drug resistance in many cancer types (Tung et al. 2012). Nevertheless, combining VEGF therapy with chemotherapy or radiotherapy yielded more promising results and was shown to have an increased effect on limiting tumor growth. This inhibitory effect shown in combining

the two therapeutic strategies was proposed to be a result of facilitated oxygen and drug delivery to the tumor tissue due to enhanced blood flow (Gilbert et al. 2014). Other anti-angiogenic therapeutic strategies that rely on interfering with the VEGF/VEGFR pathway are designed to target VEGFR2 using receptor-tyrosine kinase inhibitors (RTKI) (Olsson et al. 2006) such as Ramucirumab which is a humanized monoclonal antibody that targets the extracellular domain of VEGFR2. Using Ramucirumab gave promising results in impairing tumor growth and survival (Clarke, Hurwitz 2013).

The Notch signalling pathway is likewise a main target for anti-angiogenic therapeutic trials due to its fundamental role in sprouting angiogenesis (Mailhos et al. 2001; Patel et al. 2005). Unlike VEGF-VEGFR chemotherapeutic combined strategies that aim at neutralizing the vasculature surrounding the tumor to ease drug delivery, inhibiting Notch signalling as a tool for cancer therapy works through targeting Dll4 ligand found to be overexpressed in many cancers (Patel et al. 2005; Mailhos et al. 2001). Targeting Dll4 renders ECs more sensitive to VEGF in their microenvironment which results in a more prominent tip cell phenotype acquired by endothelial cells in the tumor vasculature that in turn leads to abnormal hypersprouting and overgrowth of blood vessels which eliminates perfusion and increases ischemia due to a more fragile, tortuous abnormal and disrupted blood vessel formation within the cancer tissue (Tung et al. 2012). Targeting tip cells characterized by high expression of Dll4 is therefore a useful approach for developing therapeutic strategies that could eliminate the adverse side effects seen as a result of interfering with normal vasculature (Siemerink et al. 2013). In one study aiming at targeting tip cells, an *in vivo* electroporation of Dll4-encoding plasmid DNA that works as a DNA vaccination against Dll4 was developed and shown to tremendously retard the tumor growth in a tumor mouse model. Injection of the Dll4-plasmid vaccine functioned by recognizing Dll4 extracellular domain and inhibiting its signalling pathway therefore resulting in impaired non-productive angiogenesis (Haller et al. 2010). In another approach, researchers modified a humanized murine antibody characterized by high specificity and binding affinity to Dll4. The modified anti Dll4 antibody denoted (H_3L_2) showed significant tumor growth suppression and reduced angiogenesis when tested both *in vivo* and *in vitro (Jia et al.*

2016). A combined therapy that works by inhibiting both Dll4 and VEGF-A was also reported to provide a promising therapeutic approach (Li et al. 2007).

From another point of view, and in another approach, a recent study that used computational modelling to study proliferation and migration in sprouting angiogenesis has implied that a balanced cooperation between these two processes is crucial for generating a more organized vasculature that covers the tumor tissue, with the overall impact of EC proliferation being more critical than the migration effect (Norton, Popel 2016). This suggested that targeting proliferation would accordingly have a more tremendous effect on inhibiting tumor angiogenesis in anti-angiogenic therapy. (Norton, Popel 2016). Nevertheless, this should be taken into consideration with accumulating data suggesting that starving tumor cells by destroying tumor vasculature could in fact result in metastasis and more aggressive cancer growth (Casanovas 2012) compared to increasing evidence that vessel normalization which results in more oxygenation and perfusion of tumor vessels is more effective in treatment due to facilitated cytotoxic drugs delivery (Carmeliet, Jain 2011b).

Taken all together, having a clear understanding of the exact processes of angiogenesis is requested for developing pharmacological agents capable of specifically and differentially targeting defined processes or pathways to effectively reduce pathologic vascular growth.

1.3 Embryonic stem (ES) cells as a model for sprouting angiogenesis

Studying the process of vessel formation and development is highly dependent on establishing the right *in vitro* vascular model (Jakobsson et al. 2007). Isolated primary EC lines have been exploited in many experiments aiming to study the process of vessel formation. For example, studies using human umbilical vein endothelial cells (HUVEC) were crucial for our present understanding of the role of ECs (Jaffe et al. 1973). However, heterogeneity of EC lines that comes up from different EC line sources limits the chances for standardized and consistent experimental studies (Kaur, Dufour 2012). Moreover, primary cell lines normally die after a certain number of passages. They also start to lose

their primary properties with time (Kaur, Dufour 2012). Immortalized EC lines on the other hand provide more reproducible outcomes (Maqsood et al. 2013). Nonetheless, using them to understand normal angiogenesis was encountered by the fact that they possess tumor cell properties that interfere with or even contradict the normal physiological characteristics of primary EC lines (Bouïs et al. 2001). Besides these obstacles, EC cultures lack the presence of a microenvironment that mimics the normal interconnected *in vivo* environment in which a 3-dimentional interaction between ECs and their neighbouring non ECs and matrix is critical for proper and controlled vascular development (Jakobsson 2007).

The use of murine embryonic stem (ES) cells in studying the process of vascular formation has been extensively demonstrated due to ES cells pluripotency and immortality in addition to their proven capability of differentiating into capillary like endothelium in 3D collagen gels (Jakobsson et al. 2010). By using ES cells derived from murine blastocysts, Doetschman et al. established in 1985 for the first time an *in vitro* model for EC development and differentiation (Doetschman et al. 1985). Consequently, assembly of differentiating murine ES cells into embryoid bodies (EBs) and their subsequent seeding into a 3-dimentional (3D) collagen matrix has been used in many studies to demonstrate the onset of vessel formation and development (Jakobsson et al. 2007).

The presence of a hemangioblast precursor at day 3 of differentiation marks the beginning of vasculogenesis. This common endothelial and hematopoietic precursor stage is followed by further differentiation into EC precursors, termed angioblasts and the formation of a primary vascular plexus (Jakobsson et al. 2007). Around day 6 of differentiation, sprouting angiogenesis occurs and the newly formed primary plexus starts to be remodelled and pruned. In collagen gels, sprouting angiogenesis proceeds in an invasive 3D manner in which newly formed vessels grow and elongate mimicking the same *in vivo* characteristics; this includes migration of vessels guided by filopodia-contained tip cells, proliferation of stalk cells, subsequent branching and lumenization, fusion of vessels, and stabilization by recruitment of perivascular cells and the

generation of a basement membrane (Potente et al. 2011; Jakobsson et al. 2007). All these are features shared between EBs grown in 3D collagen cultures and normal angiogenesis taking place *in vivo*. In this context, it is also worth mentioning that the preferential differentiation of EBs towards the vascular fate is further triggered by providing the growing ES cells with VEGF-A (Jakobsson et al. 2007).

By creating this remarkable EB *in vitro* model that emulates sprouting angiogenesis *in vivo*, it became much easier to study and understand the exact roles of different types of ECs and the pathways involved. Moreover, generating genetically manipulated ES cells is a fundamental approach by which a better understanding of the processes involved in vessel formation can be achieved. For example, competition studies are based on generating chimeric EB systems that contain both wildtype and mutant ES cells and further comparing their morphological and functional differences (Jakobsson 2006, jakobsson 2010). To further evaluate and confirm results *in vivo*, ES cells can also be introduced into the mouse system by injecting cells subcutaneously to generate teratomas which are known to give rise to various cell types including the EC lineage (Gerecht-Nir et al. 2004). Importantly, injected ES cells were found to connect to the host vasculature and contribute to the vessels contained within the generated teratomas (Gerecht-Nir et al. 2004; Li et al. 2009).

1.4 Haploid embryonic stem (ES) cells as a powerful genetic tool

1.4.1 Generation of mammalian haploid ES cells

The generation of haploid ES cells from parthenogenetic mouse embryos was a key achievement in genetic analysis and forward genetic screening (Elling et al. 2011; Leeb, Wutz 2011). Since all mammalian somatic cells are diploid, i.e. have two copies of each of their somatic chromosomes, mutations in their genome can be obscured by the presence of a normal un-mutated allele counterpart. Simpler organisms such as yeast can be haploid and hence have a single set of chromosomes (Elling et al. 2011). This has been exploited and yeast has been extensively used as a tool for studying fundamental

biological processes such as the cell division cycle where multiple temperature-sensitive cell division cycle (cdc) mutants were identified and characterized in *Saccharomyces cerevisiae* (Hartwell et al. 1973). Based on this, haploid mammalian ESCs could be successfully generated by the activation of parthenogenetic mouse oocytes, the subsequent isolation of blastocysts, and finally FACS purification of haploid ES cells and the expansion of the resulting population. Subsequent studies performed using these haploid mouse ESCs proved that they are capable of differentiating *in vitro* and *in vivo* into all three germ layers and that these cells can maintain haploidy for several passages (Elling et al. 2011; Leeb, Wutz 2011).

1.4.2 Mutagenesis of haploid ECSs

Gene traps have been widely utilized to create libraries containing single gene mutations of mouse embryonic stem cell lines that could be further used to generate mutant mice (Schnütgen et al. 2008). In the same way, mouse haploid ESCs could be mutagenized using retroviruses containing reversible gene traps that have the ability to mutate and simultaneously report gene expression in the random sites where the vector insert resides (Elling et al. 2011; Schnütgen et al. 2008).

Gene traps can be designed in many ways: one of the most commonly used designs is based on the presence of a reporter and/or a selective marker that lacks a promoter and is flanked by a 5' splice acceptor site (SA) upstream, and a 3' ploy-A sequence downstream. The lack of a promotor leads to the transcription of an inserted gene trap with the help of the endogenous promotor. When a gene trap is inserted into an intron, the resulting gene transcript contains the upstream exons spliced to the reporter and/or the selective marker due to the presence of a SA site. On the other hand, the presence of a ploy A in the downstream end of the gene trap leads to termination of transcription which results in a premature transcript that encodes for a truncated protein that is usually biologically non-functional, along with the reporter and/or the selective marker (Schnütgen et al. 2008).

A very useful application of gene trapping could be achieved by modifying gene traps in a way that enables conditional transgenesis, while allows for time and tissue specific control of gene function (Nagy 2000). Trap modification can be achieved by insertion of specific recombinase recognition sites that flank the gene trap cassette. Recombinases therefore mediate site specific recombination at those specified sites. This causes modification of the gene trap determined by the orientation of the recognition sites. If the trap vector is flanked by recombination sites both in the same orientation, this leads to the excision of the gene trap upon recombinase addition. If the gene trap is flanked by recombination sites that go in opposite orientation, this on the other hand results in the inversion of the trap cassette upon recombination which allows conditional gene disruption (Schnütgen et al. 2005; Nagy 2000). Among the most commonly used recombinase-recognition site pairs is Cre-lox recombination. Cre recombinase is a 38kDa protein that belongs to the integrase family members of site-specific recombinases. It is derived from the P1 Bacteriophage and is capable of catalysing site-specific recombination between its two (loxP) recognition sites; each of these sites consists of a 13 bp palindromic sequence, to which Cre-recombinase binds, and an 8 bp region that separates the two 13 bp sequences (Nagy 2000; Semprini et al. 2007).

In recent years, Elling et al. modified a genome-wide reversible homozygous mutagenizing system that aimed at ultimately covering the whole mouse genome and is by now covering more than 70% of annotated mouse genes. This powerful system called the Haplobank is based on randomly mutagenizing haploid ES cells to give rise to stable homozygous mutations (Elling et al. 2011; Elling et al. 2017).

1.5 Project outline

In this project, we aimed at identifying novel regulators of angiogenesis and to explore their proposed influence on tip cell specification by performing *in vitro* and *in vivo* experimental studies. For this purpose, we took advantage of two available approaches that could be combined to develop a testable, robust and reliable sprouting angiogenesis model; the first was by using the power of ES cells known for their

unlimited expansion ability and their potential to give rise to different tissue types (Nagy, Vintersten 2006). The second technology that we implemented was via utilizing murine ES cell lines homozygously targeted with repairable gene traps; these manipulated ES cells were generated by the previously mentioned Haplobank (www.Haplobank.at) (Elling et al. 2011; Elling et al. 2017).

Our approach was to test the effect of disrupting pre-selected gene candidates to identify novel angiogenesis regulators. By using our in-house Haplobank, we obtained the available ES cell clones that harbour gene trap insertions capable of impairing the function of our genes of interest. A key feature of the gene trap insert within these mutated ES cell clones is their ability to be reversed. Therefore, for each ES cell clone carrying a gene trap mutation in sense direction, a corrected version could be generated by flipping the inserted gene trap from sense to anti-sense direction using Cre-recombination. This abolishes the effect of the gene trap insert which leads to intact mature mRNA transcripts. The resulting repaired clone that represents the undisrupted sister clone will be referred to in our study as the "wildtype" counterpart. Similarly, gene traps originally located in an anti-sense direction (no disruption effect) could be activated when inverted by Cre recombinase which results in the mutant version of the candidate gene (gene trap in sense).

2 Results

Studying angiogenesis using haploid murine ES cells accompanied by a conditional mutagenizing system enabled us to perform loss-of-function *in vitro* and *in vivo* experiments to identify novel regulators of angiogenesis by generating wildtype-mutant sister clone pairs for each candidate gene. Therefore, we could directly and reliably assess the effect of disrupting a specific candidate gene by using the exact same clone batch as a wildtype and a mutant source which excluded any possible effect of varied clone differences that might interfere with the resulting phenotypes (Elling et al. 2017).

2.1 Defining candidate genes for functional analysis studies

Choosing the candidate genes was based on two previous studies that aimed at inspecting both, genes enriched in murine wildtype retinal tip cells (Strasser et al. 2010), and genes up or down-regulated in retinal tip cells of *Dll4*$^{+/-}$ mouse mutants (del Toro et al. 2010). The following 8 genes were directly selected from these two lists and examined in the first round of our experiments: *Enpp3*, *Ndufs4*, *Plcb1*, *Syt16*, *Tesc*, *Igfr1*, *Prkcz* and *Myst3.*

Using the ingenuity software, we further used the gene lists of Strasser and del Toro studies to choose the genes that in clinical studies were recorded to be associated to vascular disease in human. Table 1 shows the selected Strasser and del Toro genes shown to be implicated in human vascular disease studies along with the corresponding number of reported citations.

Of note, we were limited to choose genes whose mutated versions were available in the in-house Haplobank. From the existing genes, we only chose the ones that harboured the insertional gene traps within the first two introns, preferably and in most cases

within the first intron to ensure disruption of the desired gene. This yielded 24 genes highlighted in yellow in Table 1.

In total, 32 gene candidates were eventually chosen.

del Toro			
Genes in dataset	Findings	Genes in dataset	Findings
F2	84	*Cdh13*	3
Ptgs1	52	*Cd40*	3
Tgfbr2	43	*Abcb1*	3
Acvrl1	34	*Tnfsf10*	2
Tfpi	30	*Timp3*	2
Angpt2	19	*Smarca1*	2
Serpine1	16	*S100b*	2
Pdgfrb	12	*Mapt*	2
F3	11	*Lyn*	2
Cav1	11	*Lcp1*	2
Ctss	10	*Irf8*	2
Thbd	9	*Gabra5*	2
Tlr2	7	*Gabra3*	2
Itgam	7	*Fcgr1a*	2
Il1b	7	*Cxcl2*	2
Ccl2	7	*Casp8*	2
Cxcl10	6	*Capg*	2
Abcg2	6	*B2m*	2
Tnfrsf1a	5	*Arhgdib*	2
Prkch	5	*Vsnl1*	1
Col1a1	5	*Vim*	1
Tnfrsf11b	4	*Ssbp2*	1
Tes	4	*Slco2a1*	1
Pdgfb	4	*Rgs1*	1
Hspg2	4	*Rcsd1*	1
Fos	4	*Rasgrp3*	1
Flt1	4	*Prr16*	1
F2r	4	*Prcp*	1
Entpd1	4	*Nox4*	1
Ackr3	4	*Mecom*	1
Zfp36	3	*Hpgd*	1
Slc16a6	3	*Fut4*	1
Procr	3	*Ets2*	1
Plaur	3	*Dlg2*	1
Pf4	3	*Cxcl3*	1
Ly96	3	*Col18a1*	1
Klf2	3	*Ccl3l3*	1
Hcls1	3	*Bag3*	1

Gja1	3	*Anxa2*	1
Gabrb3	3	*Adm*	1
Gabrb2	3	*Abcc9*	1
Strasser			
Genes in dataset	Findings	Genes in dataset	Findings
VEGF-A	53	*Cfhr1*	2
Angpt2	19	*Cxcr4*	2
Il1b	7	*Hck*	2
Igf1	5	*Irf8*	2
Itgav	5	*Pde4b*	2
Ackr3	4	*Col2a1*	1
Bmp7	3	*Disp1*	1
Grin2b	3	*Gfod1*	1
Mtor	3	*Pcsk6*	1
Slc16a6	3	*Vldlr*	1

Table 1: Defining gene candidates for sprouting angiogenesis.
Genes enriched in retinal tip cells (Strasser list) or differentially up or down regulated in *Dll4* heterozygous mouse retina (del Toro list) ranked by their frequency of reported citation in human vascular disease. Genes found available with a 1st or 2nd intron gene trap insertion in the Haplobank are highlighted in yellow.

2.2 Validation of Haplobank clones

After obtaining the haploid ES cell clones with the desired gene traps from the Haplobank, we sought to validate the identity of each clone before starting the sprouting assays. Every gene trap vector engineered by the Haplobank was originally designed to contain a 32 bp-unique barcode which is located downstream of the long terminal repeats (LTR). Moreover, all vectors were optimized to contain a common primer binding site that enables the amplification of the specified barcode of each clone using the same PCR protocol. Based on this unique design of the trap vectors, we validated each obtained clone by performing a PCR that amplified the barcode of each tested clone. Subsequently, we performed Sanger sequencing to align and compare the amplified barcodes to the ones identified and mapped by the Haplobank for each gene trap. If deviation from the original barcode sequence was noticed, then that was an indication that either it was a different clone, or that the clone carried multiple gene traps. In both cases, those clones were excluded from our study (Figure 2.1 A-C).

A

Cell Information

Cell ID:	00341IE06	
Gene:	Ets2	
Mutation:	1Intron	
Rel. Orientation:	sense	
Synonyms:	Ets-2	
Strand of Integration:	+	
Mutagen:	Lenti-EGT	
Genomic Location:	chr16:95717686	
Barcode:	ACTCTCTCACACACACACTGACAGTGTGACAC	17470
Sequence:	AGGAGCCACTGTCCACTCCCTTCCCTACCCACTAGGCTTCCAAGAGGATG	18866
RPKM:	44	
PerfectGT:	★	
Quality Control:	●●●	
Description:		
Amount:	€150.00	

B

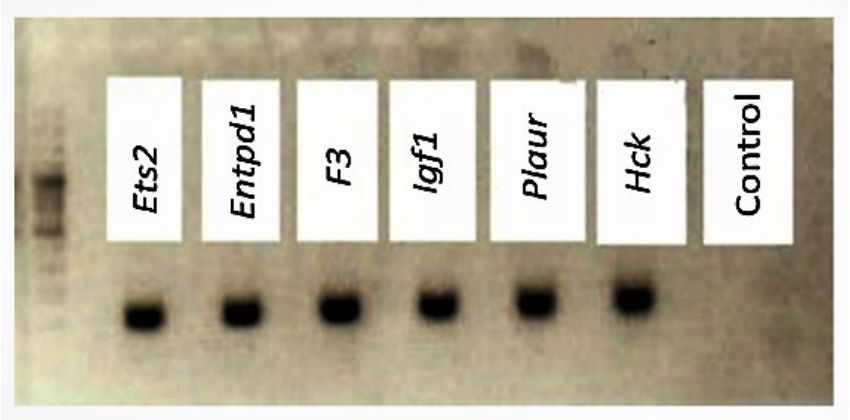

C

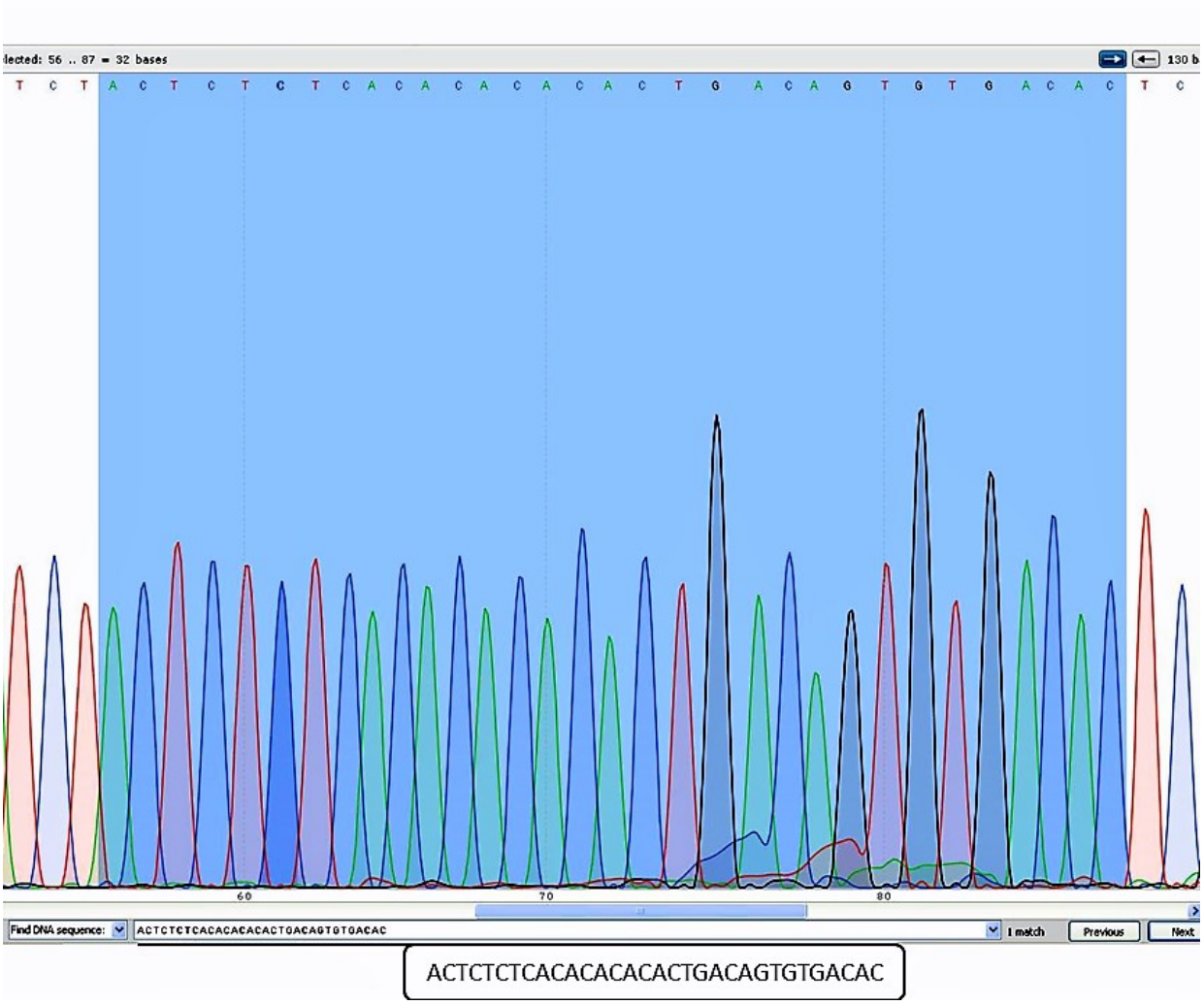

Figure 2.1 Verification of haploid ES cell candidate clones obtained from the Haplobank by barcode PCR and Sanger sequencing.

A A representative example of a candidate clone that harbours a gene trap within the *Ets2* gene. Information about *Ets2* gene trapping from the Haplobank demonstrates a first intron-gene trap insertion in sense direction (www.haplobank.at). **B** A gel electrophoresis image for barcode PCR showing the bands of some selected candidate genes including the *Ets2* gene. **C** Validation of *Ets2* gene by matching the *Ets2* barcode sequence amplified by PCR (ACTCTCTCACACACACACTGACAGTGTGACAC) with its corresponding sequence given by the Haplobank to verify clone identity:

```
Derived barcode:     A C T C T C T C A C A C A C A C A C T G A C A G T G T G A C A C
                     I I I I I I I I I I I I I I I I I I I I I I I I I I I I I I I I
Reference barcode:   A C T C T C T C A C A C A C A C A C T G A C A G T G T G A C A C
```

2.3 Cre recombinase-mediated gene trap flipping and tagging of wildtype and mutant haploid ES cell sister clones

After verifying the different candidate clones obtained from the Haplobank, our next step was to generate a mirrored clone representing the wildtype control or the mutant version for each of the clones that we aimed to study. As mentioned above, Cre-mediated inversion of the gene trap from sense to antisense direction repairs the mutation and accordingly renders the gene's ability to undergo normal gene splicing and expression, and vice versa (Elling et al. 2017) (Figure 2.2) . To apply this on our list of candidate clones, we aimed at producing two types of ecotropic retroviruses by transfecting Platinum-E cells (Plat-E Cells). The first was produced by transfecting Plat-E cells with retroviral constructs containing CRE recombinase conjugated to a red fluorescent construct (m-Cherry) which worked as a marker that tagged the flipped clones. The other ecotropic retrovirus type was produced using a GFP construct in order to mark the clones carrying the gene trap in its originally inserted orientation in green.

Marking the sister clones with m-Cherry or GFP was essential for subsequent competition assays (Jakobsson et al. 2010). Importantly, the two retroviral constructs harboured in addition a puromycin resistance cassette to select for ES cells that in deed integrated the plasmid in their genome. 48 hours following Plat-E cells transfection, supernatants including the produced retroviral particles were collected, filtered and stored at -80°C for later infection of haploid ES cell clones. Each candidate clone obtained from the Haplobank was thawed, expanded, and separated into two groups subsequently infected with ecotropic retroviruses carrying either CRE m-Cherry or GFP. Following (48) hours of infection, we started using a selection medium containing puromycin to deplete all cells that did not integrate the plasmid which resulted in a pure population of cells expressing either GFP or Cre- m-Cherry. Thus, we have developed a system that allows to reliably revert the insertion vectors and generate mutant and wildtype sister clones with red or green colour tags.

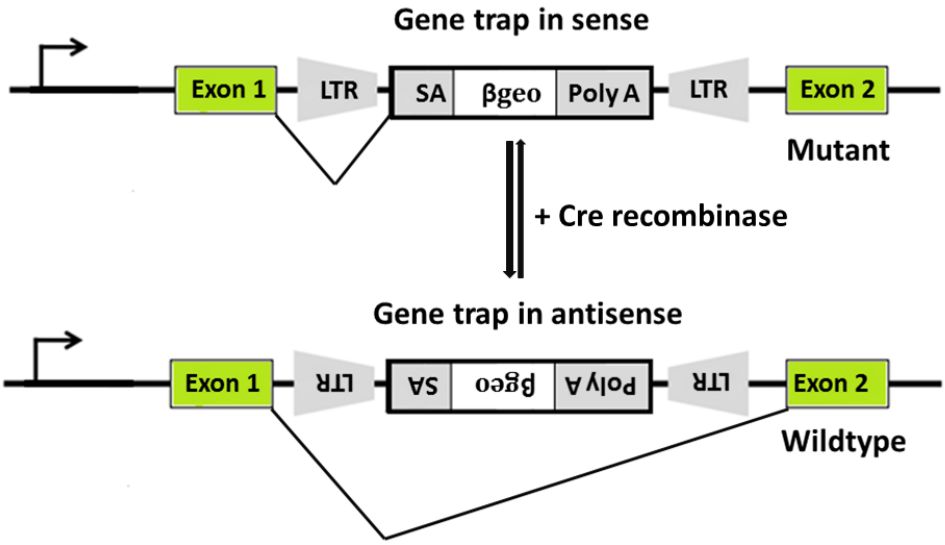

Figure 2.2 A schematic representation of Cre recombinase-mediated gene trap flipping.

Haploid ES cells infected with retroviruses carrying a CRE m-Cherry construct were reverted into WT or mutant cells depending on the original orientation of the gene trap insert. LTR: long terminal repeats, SA: splice acceptor, β-Geo: galactosidase and neomycin resistance gene, Poly A: Polyadenylation (stop) signal**.** Adapted from (Elling, Penninger 2014).

2.4 Isolation of fluorescent haploid ES cells

Many reports pointed to the observation that exogenous genes in ES cells undergo silencing (Cherry et al. 2000). Although gene silencing in ES cells early in development is an endogenous hallmark feature required for gene regulation and imprinting and also as a defensive mechanism against viral infection, it also poses an obstacle for genetic studies that aim to incorporate vectors into the ES cell genome and seek a long term stable expression of the exogenous genes (Rival-Gervier et al. 2013). To overcome this problem in our infected clones, we used fluorescence-activated cell sorting (FACS) to isolate groups of cells that showed the highest expression of the inserted constructs reflected by the highest fluorescence. Accordingly, the highest ~ 5% fluorescent cells of each population were isolated, obtained and expanded under constant puromycin selection pressure to be used in subsequent experiments (Figure 2.3).

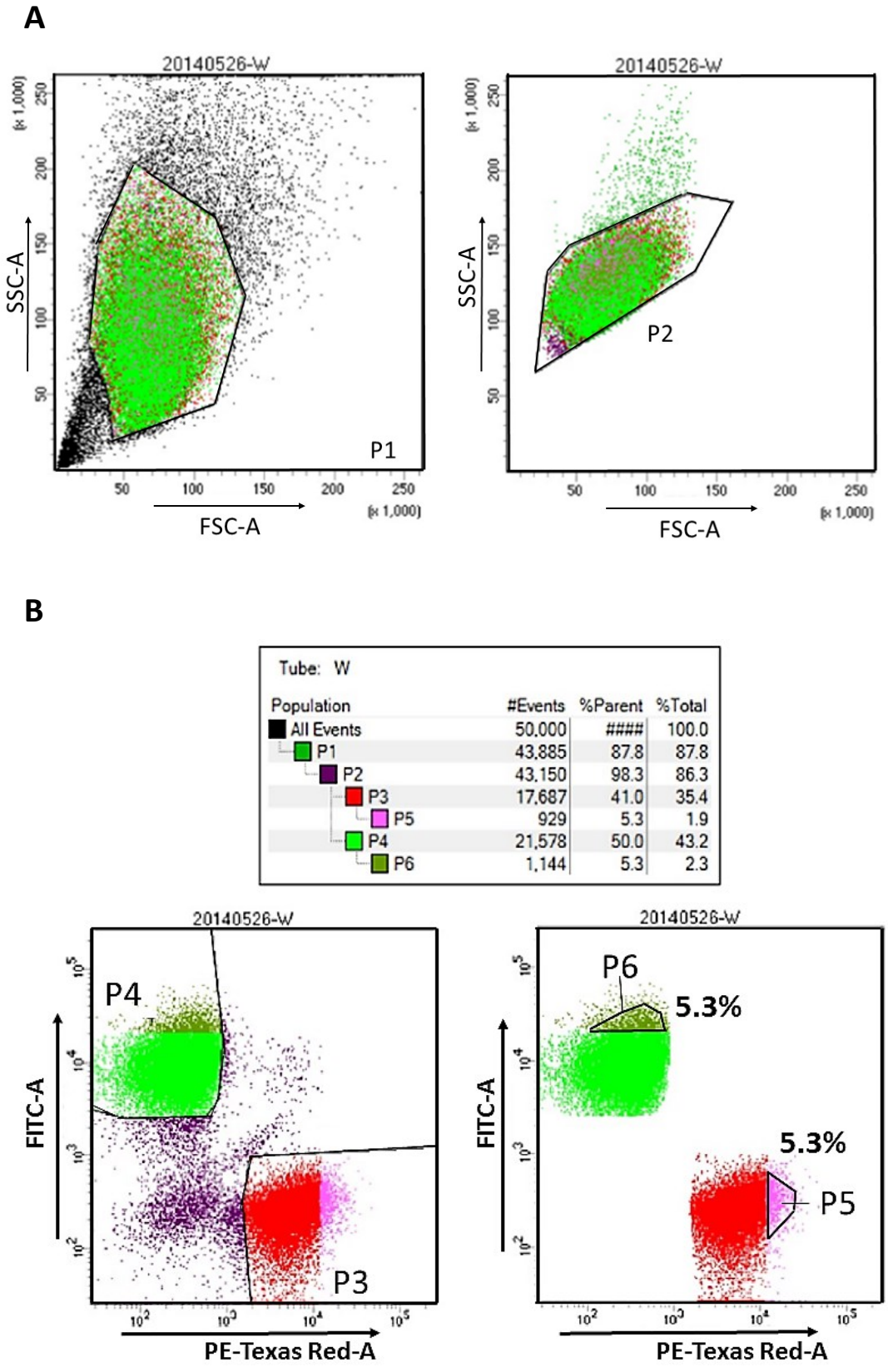

Figure 2.3 A representative example for sorting GFP and CRE m-Cherry highly fluorescent cells by FACS. **A** ESC populations were defined by light scattering (FSC and SSC) and gated for single cells (P2). **B** Sorting of cells based on their fluorescence; (P3) represents the population of cells with m-Cherry fluorescence

and (P4) represents the population of cells with GFP fluorescence. (P5) and (P6) represent the ~ 5% highest fluorescent cells from each population, respectively. This fraction of cells was obtained and further expanded.

2.5 Sprouting angiogenesis of embryoid bodies (EBs) in 3D collagen matrix.

To functionally evaluate the importance of our candidate genes in sprouting angiogenesis *in vitro*, we adopted a 3-dimensional collagen sprouting assay using embryoid bodies (EBs) generated from haploid ES cells of each candidate clone. Growing these organoids in a 3D collagen matrix enabled them to recapitulate many key properties of angiogenesis featured in *in vivo* (Jakobsson et al. 2010).

In order to achieve this, the following approach was applied on all the 32 candidate clones in our list: FACS sorted highly fluorescent cells were cultured and further expanded under puromycin selection pressure for a few days until they reached confluency. We used GFP and CRE m-Cherry haploid ES cells of each clone to generate EBs using low attachment 96-well plates in the absence of LIF. Our approach was to generate three sets of EBs for each candidate clone that we wanted to study, one set was made of haploid ES cells from the wildtype clone only (antisense clone), and the other set was made of the mutant sister clone only (sense clone). The aim of generating these two sets was to directly compare their sprouting capacities and to evaluate the effect of mutating the gene of interest on vessel formation. The third set was a 1:1 mixture designed to generate mosaic EBs made of equal numbers of wildtype and mutant haploid ES cells. The idea behind this setup was to assess the competition between wildtype and mutant clones for acquiring the leading tip cell position in the growing sprouts (Jakobsson et al. 2010).

After approximately 8 days, we embedded the generated EBs in a collagen matrix and stimulated endothelial differentiation with 50ng/mL VEGF-A. This led to a robust and very reproducible outgrowth of vessel like structures. After sprouting for approximately 10 days in 3D collagen matrix, we examined the grown vessels using a bright field

microscopy for a general assessment. We subsequently fixed the EBs and immune-labelled them using IB4 or CD31, both specific endothelial cell markers (Elling et al. 2017). All EBs representing the wildtype and the mutant clones were then imaged and the sprouts of each candidate clone were manually quantified to assess the influence of gene disruption on angiogenesis. Competing mosaic EBs were examined using confocal microscopy to evaluate tip cell competition by counting the percentages of GFP or m-Cherry positive cells at the tip position of the generated vessels.

2.5.1 AN3 haploid ES cells stably expressing GFP and CRE m-Cherry show equal sprouting capacity and similar tip cell dominancy

AN3 represents the original haploid ES cell sub-clone that was chosen to generate the Haplobank as it was shown to exhibit a rapid and robust growth on feeder-free conditions, maintain a haploid and stable genome over many generations and can differentiate into all three germ layers (Elling et al. 2011, 2011; Elling et al. 2017). Therefore, we used AN3 cells as a control in our study. For this purpose, we started our *in vitro* sprouting assay experiments by testing GFP and CRE m-Cherry infected AN3 haploid ES cells for their ability to sprout and form vessels when cultured in a collagen matrix gel. We further investigated whether stably infecting haploid ES cells with CRE would influence the sprouting capacities of haploid mouse ES cells. Following the same approach described above for EB formation and the collagen matrix sprouting assay, we generated AN3 EBs of GFP, CRE m-Cherry, and mosaic 1:1 GFP:CRE m-Cherry-cells and cultivated them in 3D collagen matrix.

Our results showed that all AN3 EBs were capable of sprouting and forming vessel like networks. The emerging outgrowths of the EBs stained positive for the endothelial marker Isolectin B4 (IB4) which confirmed the vascular origin of the outgrowth (Figure 2.4 A). By comparing the average number of sprouts formed by GFP and CRE m-Cherry infected EBs, our results also indicated that there was no apparent difference in the sprouting capacities between the two sets of AN3 EBs (Figure 2.4 B). Therefore, infecting haploid ES cells with retroviruses containing GFP or CRE m-Cherry constructs had no

apparent effect on the endogenous ability of haploid ES cells to differentiate into ECs and undergo vessel formation.

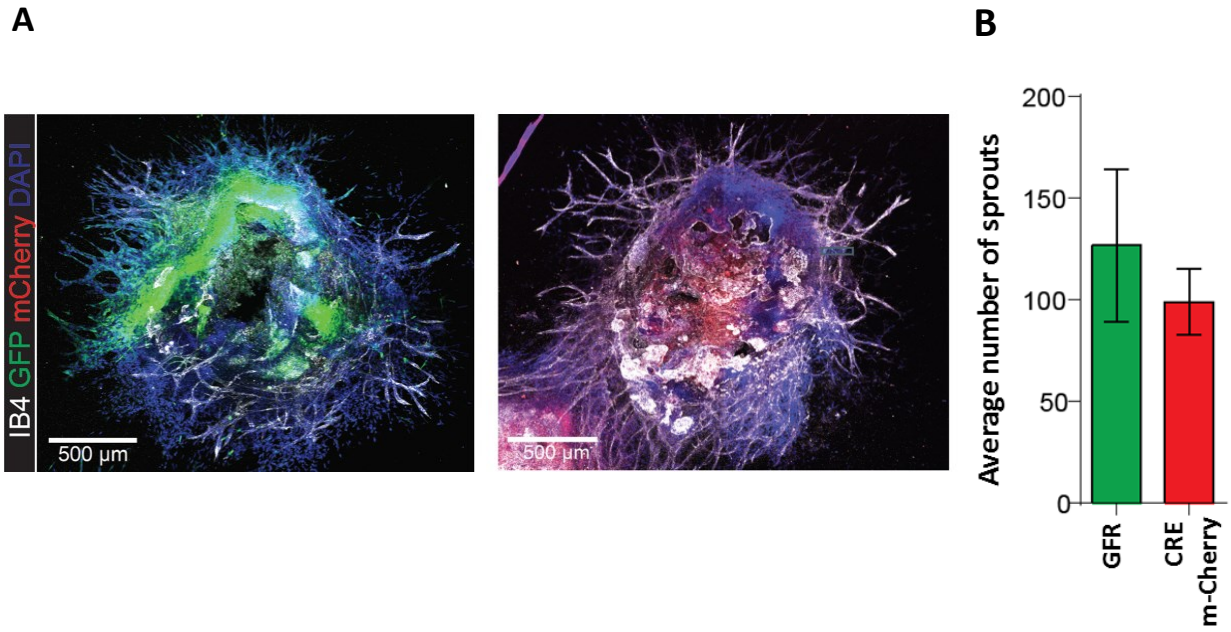

Figure 2.4. Generation of an *in vitro* angiogenic model using stably expressing GFP or CRE m-Cherry control haploid ES cells.
A The *in vitro* sprouting ability of EBs derived from AN3 haploid ES cell clones retrovirally infected with either GFP (left) or CRE m-Cherry (right) was assessed: Vessels were marked by IB4. DAPI counterstain was used to mark cell nuclei. **B** Comparison between the numbers of vessels quantified for both GFP-expressing and CRE m-Cherry-expressing AN3 EBs didn't show an apparent difference in their sprouting capacities. Data represents mean numbers of $IB4^+$ blood vessels ± SEM of >8 EBs from 2 independent experiments. Students t-test P=0.316

To further confirm that GFP and CRE m-Cherry AN3 infected cells possess the same ability to sprout and have the same chances in undergoing the tip cell fate, we examined the mosaic EBs, representing a 1:1 GFP, CRE m-Cherry cell mixture, for tip cell dominancy. Tip cells were identified by their position in the leading front of the growing sprouts and by their morphology. The identity of tip cells was determined by their green or red fluorescent signals (Figure 2.5 A, B). By comparing the number of tip cells occupied by either GFP or CRE m-Cherry haploid ES cells, we concluded that the two fluorescent

clones have an equivalent efficacy towards tip cell specification. Therefore, acquiring the tip cell position was not influenced by the construct type inserted into ES cells.

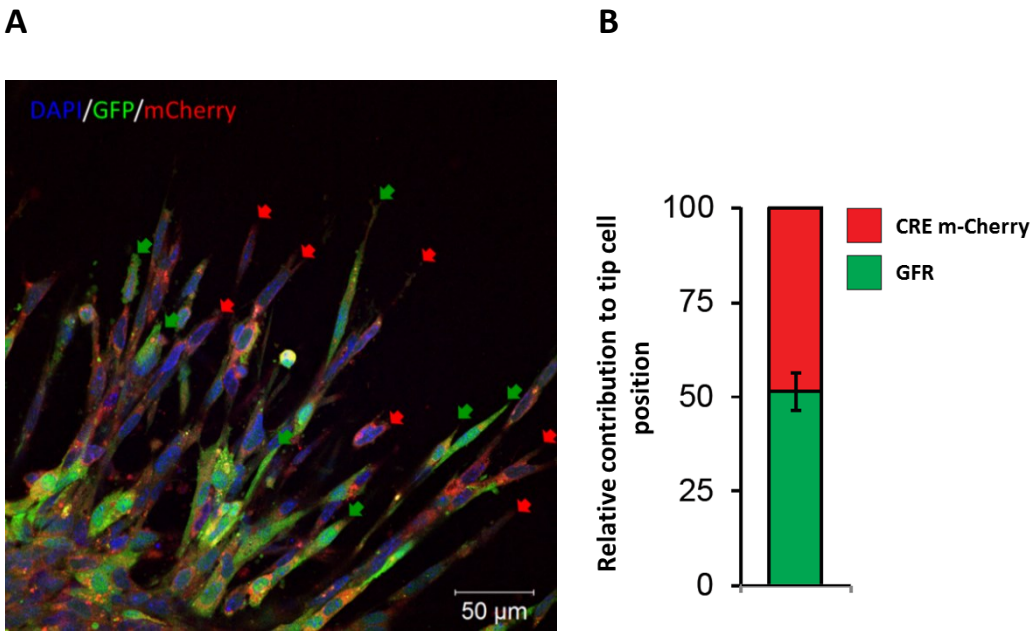

Figure 2.5 GFP and CRE m-Cherry-expressing control haploid ES cells showed an equal contribution to the tip cell position in the competition assay.
GFP and CRE m-Cherry 1:1 mosaic AN3 EBs contribute equally to the tip cell position (51.5 % GFP^+; 48.5 % CRE m-$Cherry^+$) which excluded any possible influence of the inserted constructs on the endogenous ability of haploid ES cells to become tip cells. Data represents mean values +/- SEM analysing >12 EBs generated in 2 independent experiments

In conclusion, haploid ES cells are capable of sprouting and forming ECs in 3D collagen matrix assays. Importantly, infecting haploid ES cells with retroviruses leading to GFP or CRE m-Cherry construct insertion has no influence on the cells ability to sprout and to acquire the tip cell position.

2.5.2 Identification of novel regulators of sprouting angiogenesis

In order to discover novel regulators of angiogenesis we evaluated the effect of disrupting each candidate gene in our list on sprouting angiogenesis. We applied the described 3D collagen matrix assay on each candidate gene separately and compared the resulting phenotypes of wildtype vs. mutant sister cells.

Figure 2.6 shows a representative example of one candidate clone (*Enpp3*). Generated EBs of wildtype and mutant sister clones were embedded in separate collagen gels to generate sprouts for around 10 days. Vessels were visualized using endothelial specific IsolectinB4 (IB4) and imaged using confocal microscopy. The number of vessels per EB was used as a measurement of sprouting capacity.

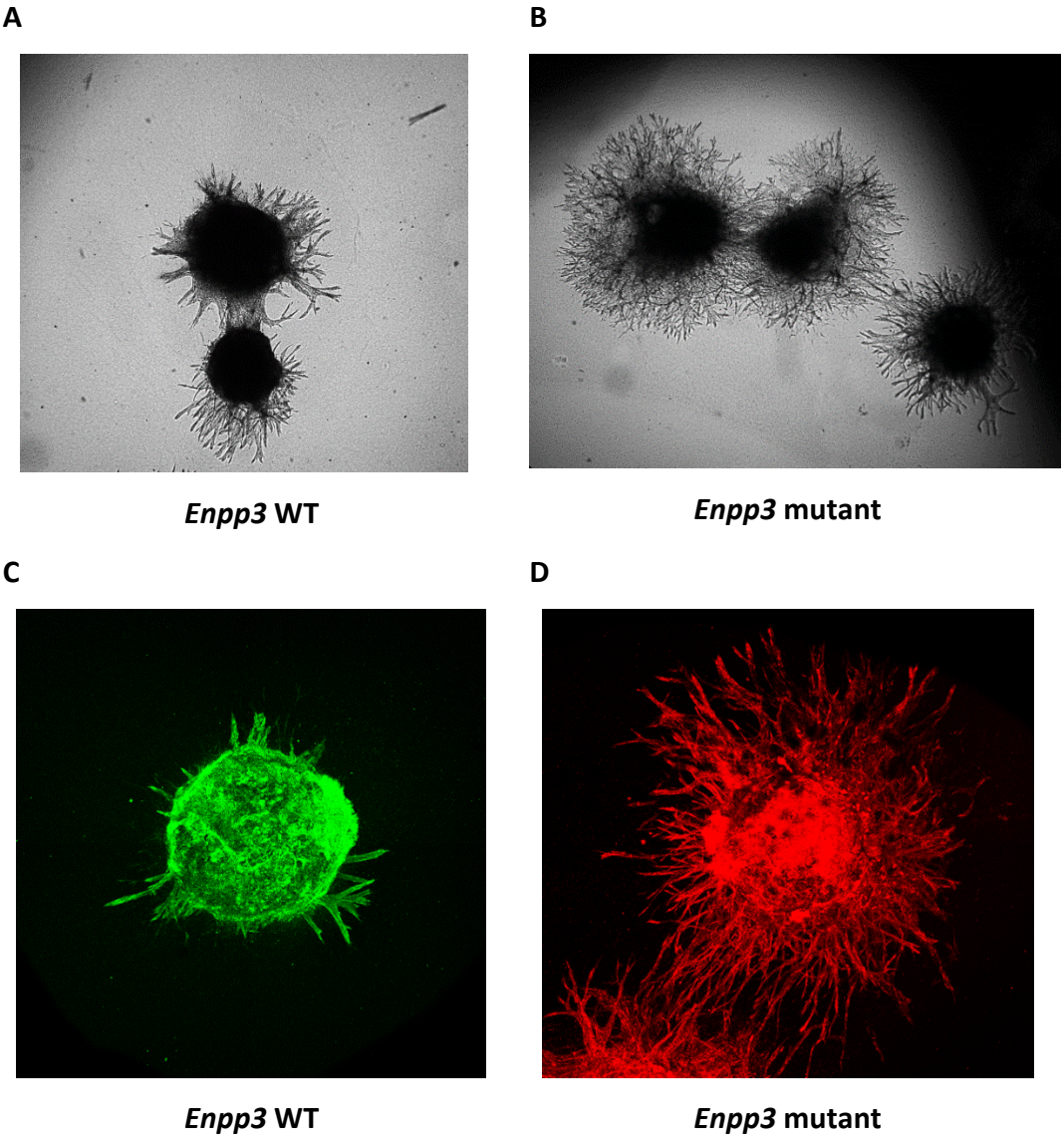

Figure 2.6 Sprouting angiogenesis in wildtype vs. mutant clones.
Wildtype and mutant EBs of *Enpp3* candidate clone are shown sprouting in 3D collagen matrix 10 days after embedding. **A, C** Sprouting angiogenesis in wildtype *Enpp3* EBs. **B, D** Sprouting angiogenesis in mutant *Enpp3* EBs. As shown, the *Enpp3* mutant clone exhibits a hypersprouting phenotype compared to its wildtype counterpart. Images captured in bright field microscopy (A, B). IB4 was used to mark ECs (C, D).

By studying the whole set of gene candidates, our results demonstrated that disrupting certain genes significantly affected the sprouting capacity of EBs either by further driving vessel formation or by abrogating it. This was represented by a hypersprouting or a hyposprouting phenotype of mutant clones compared to their corresponding wildtype counterparts. Of a total of 32 candidate clones studied, 13 genes were shown to cause a significant change in the sprouting capacity of ES cells. The mutated forms of *Enpp3*, *Smarca1*, *Ndufs4*, *Plcb1*, and *Hck* significantly promoted blood vessel formation denoted by a higher average number of sprouts protruding from EBs compared to the un-mutated counterparts. By contrast, mutating *Myst3*, *Mecom*, *Gja1*, *Gabrb3*, *Tnfrsf1a*, *Dlg2, Grin2b and Cdh13* genes had a significant inhibitory effect on vessel formation denoted by a significant decrease in the average number of vessels compared to the corresponding wildtypes (Figure 2.7, Figure 2.8).

Of note, a key observation concluded from comparing the sprouting phenotypes of wildtypes from different candidate clones was the high variability in their endogenous sprouting capacities (Figure 2.8 B). Consequently, it was important to take this into account when comparing different candidate clones. We therefore normalized the results obtained from all the different clones to avoid false positive or false negative outcomes and to assess direct comparison of different sister clones (Figure 2.8 A).

A Hyposprouters

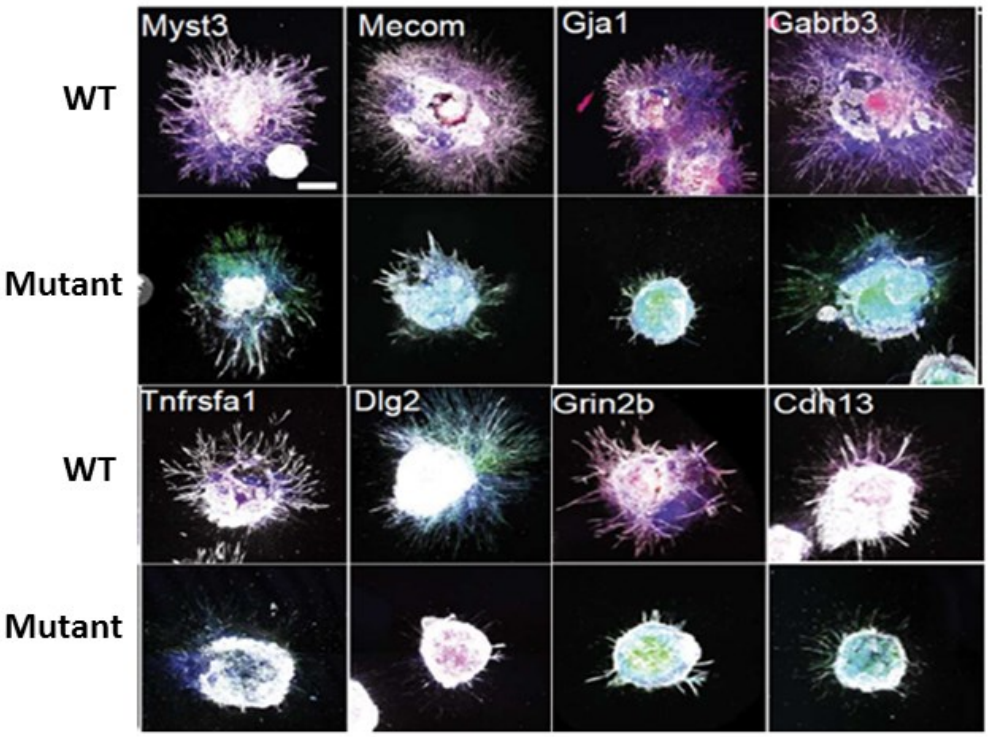

B Hypersprouters

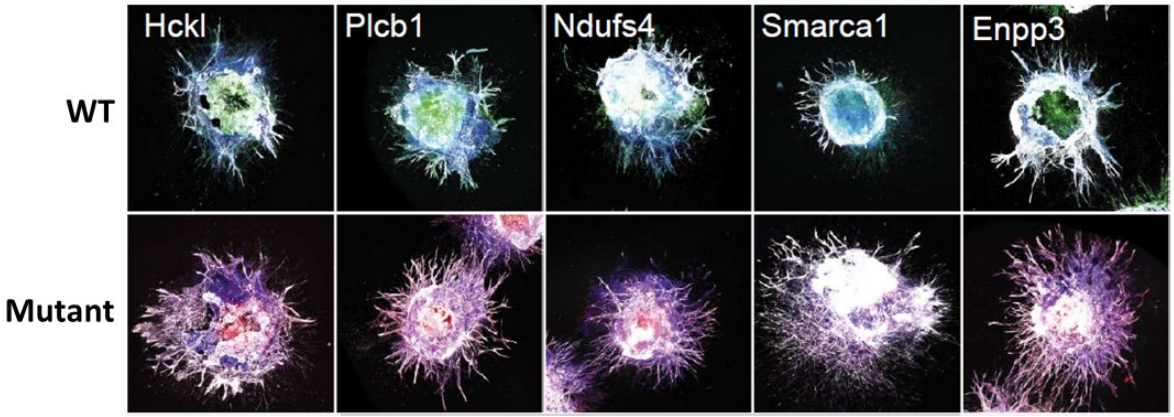

C Candidate clones with equivalent sprouting capacities

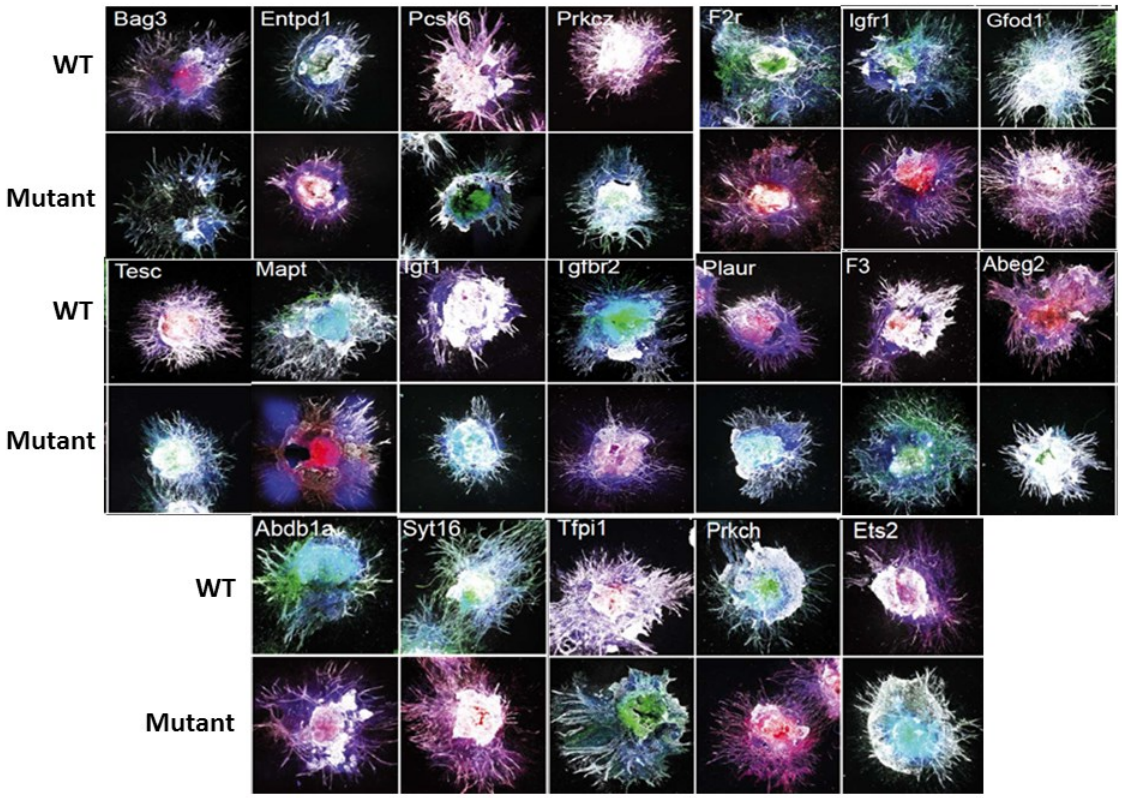

Figure 2.7 Novel regulators of sprouting angiogenesis.
3D collagen matrix assay was performed to compare the sprouting capacities of wildtypes vs. mutants for the 32 candidate clones. **A** Disruption of genes in this group of candidate clones led to a prominent impaired ability of haploid ES cells to undergo sprouting which resulted in a hyposprouting phenotype. **B** Clones harboring a mutation in this group of genes were found to exhibit an apparent increase in their sprouting capacities which led to a hypersprouting phenotype. **C** Disruption of genes in these candidate clones did not have a noticeable influence on the sprouting capacities of mutated clones compaired to their non-disrupted counterparts. ECs were marked using IB4.

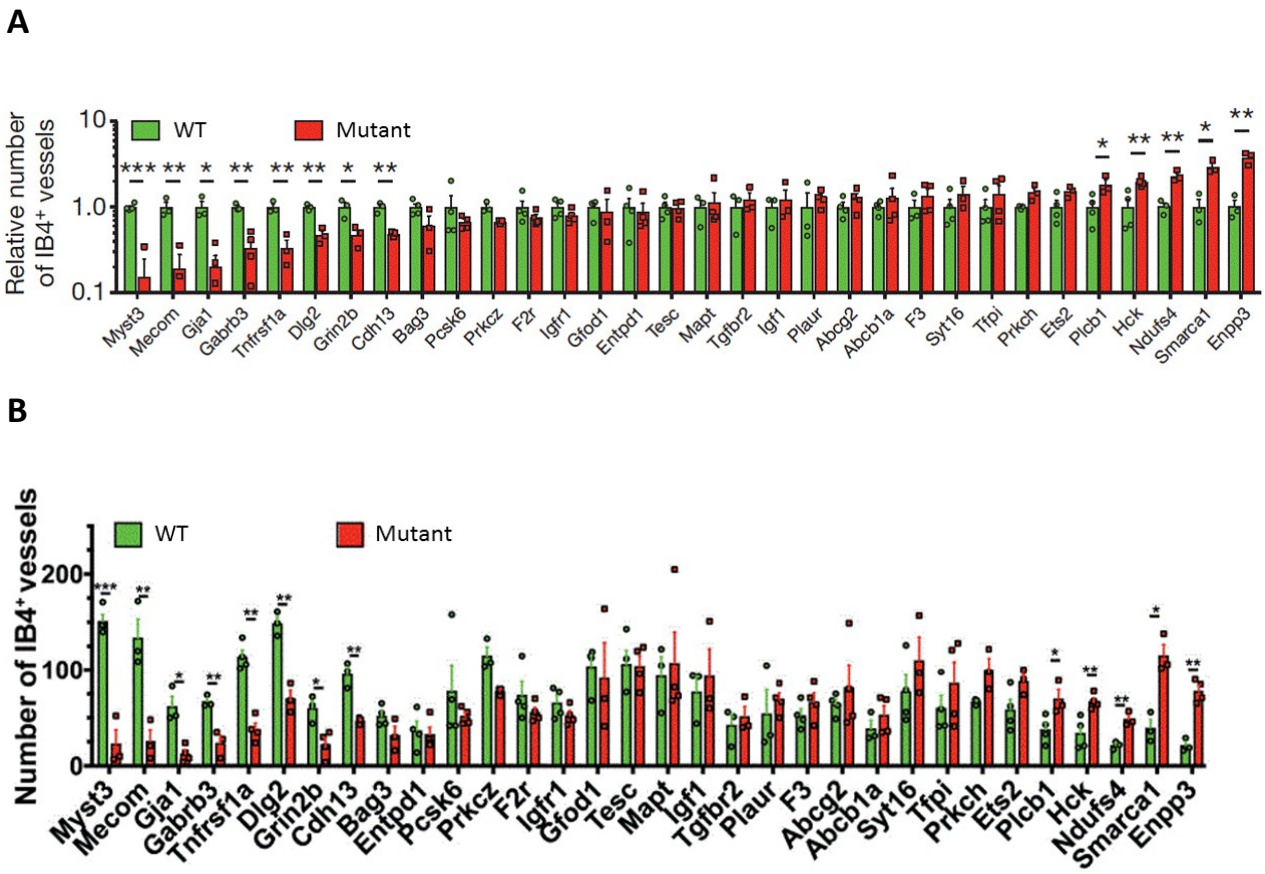

Figure 2.8 Sprouting capacities of haploid ES cell candidate clones
A Sprouting capacities of wildtype vs. mutated candidate clones based on the relative number of IB4$^+$ vessel sprouts quantified for EBs of each candidate clone. Data was normalized to the respective wildtypes of each canidate clone. **B** Quantification of sprouts for wildtype and mutant sister clones shown as un-normalized data. Note the high variability in the number of sprouts for wildtypes of different candidate clones. Data are shown as mean values ± SEM. * $P < 0.05$; ** $P < 0.01$; *** $P < 0.001$ (Students t-test). For each mutant/wildtype sister clone combination, >200 vessels were counted from 2 independent experiments.

Importantly, using an EC marker is a crucial step in our quantification procedure to verify that the outgrowths arising from EBs were indeed vessels and no other non-EC sprout-like structures. This was pivotal to obtain accurate quantification results that led to reliable outcomes. This importance was evident when studying EBs of some candidate clones which showed sprout-like structures that failed to stain positive when immunostained with the EC marker IB4. (Figure 2.9).

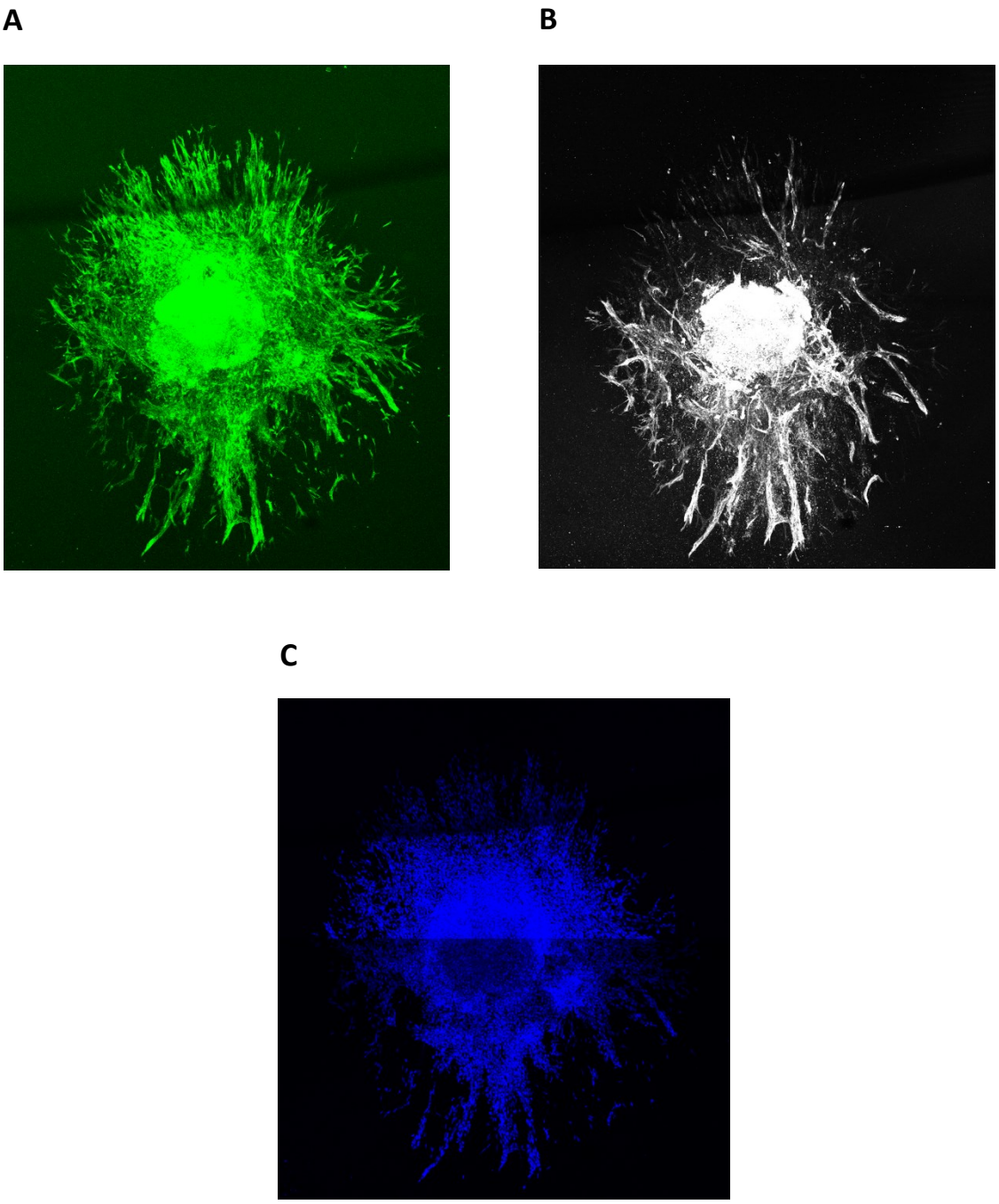

Figure 2.9 Identification of vessel sprouts using isolectin B4 (IB4) immunostaining
A representative sprouting example of the *Myst3* mutant candidate gene. EBs were assayed and stained with IB4-EC marker for quantification. The mutant *Myst3* clone harboured the gene trap in sense direction and so expresses the GFP fluorophore. **A** A sprouting EB examined by displaying the GFP fluorescence**. B** The same EB shown by displaying the IB4-EC marker only (white). **C** DAPI marker displayed for the same EB. Note the presence of both, endothelial and non-endothelial structures emerging from mutant *Myst3* EB.

2.5.3 Tip cell behaviour highly correlates with sprouting capacities

As our candidates represent genes that are differentially expressed in tip cells, we aimed to explore the ability of mutant vs wildtype candidate clones to compete for the tip cell position in 1:1 mosaic EBs. Tip cell competition models have been described previously (Jakobsson et al. 2010; del Toro et al. 2010). In our approach, we focused on the candidate clones that revealed a hyper- or hyposprouting phenotype by examining mutant/wildtype equally mixed EBs using collagen matrix assay protocol. We then examined the originating sprouts by comparing the green and red signals denoting the two sister clones for dominating the tip cell position.

With the exception of *Enpp3* which did not show a significant difference, our data showed that in general, hypersprouting gene mutants acquired the tip cell position more often when competing with an equal number of wildtype counterparts. Similarly, mutants showing a hyposprouting phenotype were found more rarely leading the growing sprouts. These observations further emphasized the competitive behaviour previously reported about tip cells (Jakobsson et al. 2010) and more importantly showed that cells possessing a higher sprouting capacity have an evident preferential dominancy for the leading tip position in competitive tip fate studies (Figure 2.10)

A

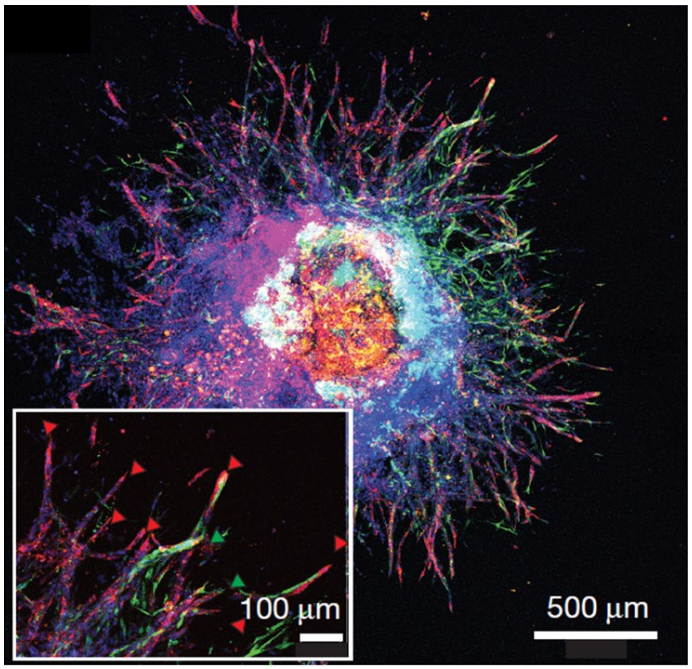

B

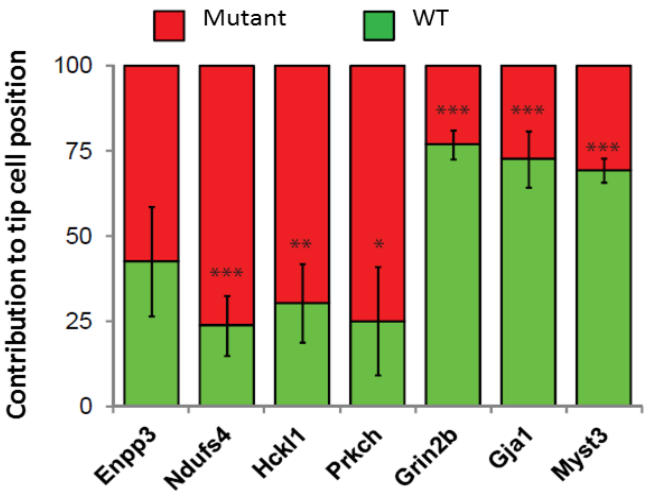

Figure 2.10 Competition of WT-Mutant candidate clones for acquiring the tip cell position.
A A representative image of mosaic sprouts from WT and mutant *Gja1* sister clones. 1:1 ratio of WT (m-Cherry) and mutant (GFP) *Gja1* ES cells were mixed to generate mosaic blood vessel. WT *Gja1* was shown to contribute more to the tip cell position in the growing sprouts compared to the mutant sister clone. **B** Relative contribution of competing wildtype and mutant sister clones to the tip cell position. Gene trapped clones showing a hypersprouting phenotype were shown to exhibit more contribution to the tip cell position when competing with their wildtype counterparts. An exception was the Enpp3 gene which didn't show a significant result. Similarly, wildtype clones competing with their hyposprouting counterparts showed an obvious tendency to possess the leading tip position. The competition assay was performed in 3D collagen matrix using 1:1 wildtype-mutant chimeric EBs. Data represents mean ± SEM of 6-8 EBs counted in 2 independent experiments for each sister clones. * $P < 0.05$; ** $P < 0.01$; *** $P < 0.001$ (Students t-test).

2.6 *In vivo* formation of a mosaic haploid ES cell-derived vasculature.

After identifying novel genes that regulate sprouting angiogenesis and tip cell behaviour *in vitro*, we aimed to confirm the importance of those genes *in vivo*. Previous published studies have shown that injection of ES cells in a mouse model results in the formation of teratomas that can give rise to various tissue types derived from all three germ layers (Gerecht-Nir et al. 2004). Importantly, vessels derived from injected ES cells were shown to contribute to and exert a physiological role in teratomas formed subcutaneously in injected mice (Bulic-Jakus et al. 2006; Li et al. 2009). Our goal was to inject immunocompromised mice subcutaneously with haploid ES cells of clones chosen from our candidate gene list shown to have a prominent effect on angiogenesis *in vitro*. GFP or m-Cherry tagging of our infected clones enabled us to distinguish between host and ES cell derived vasculature. However, since ES cells were shown to often undergo gene silencing upon prolonged periods of time (Pfeifer et al. 2002), we could detect very little reporter expression in teratomas when mice were injected with haploid ES cells in pilot studies.

EBs have previously been reported to result in teratoma formation *in vivo* following subcutaneous injection in mice (Kim et al. 2013). Therefore, I speculated that injecting already differentiated EBs that were cultured under constant puromycin selection pressure could have an advantage over injecting ES cells (Figure 2.11 A). Evidently, injected EBs in subsequent pilot studies retained their ability to express the inserted reporter constructs inferred from the fluorescence signal observed by examining teratoma tissues. Therefore, and in order to first assess the *in vivo* contribution of haploid ES cells to the vasculature in growing teratomas, we generated m-Cherry-tagged EBs derived from wildtype haploid ES cells, kept under puromycin selection and injected them subcutaneously into immunocompromised mice. Teratomas grown for 3-4 weeks were harvested, and ECs were marked using IB4 immunostaining. We were particularly interested in finding regions that revealed a co-localization of m-Cherry with $IB4^+$ ECs as this represented vessels originating from the injected haploid ES cells. Importantly, we could in deed detect regions positive for both IB4 and m-Cherry which was a proof of

principle that our haploid ES cells injected in the form of EBs contributed to teratoma vasculature and were able to differentiate into ECs and form vessels when injected *in vivo* (Figure 2.11 B)

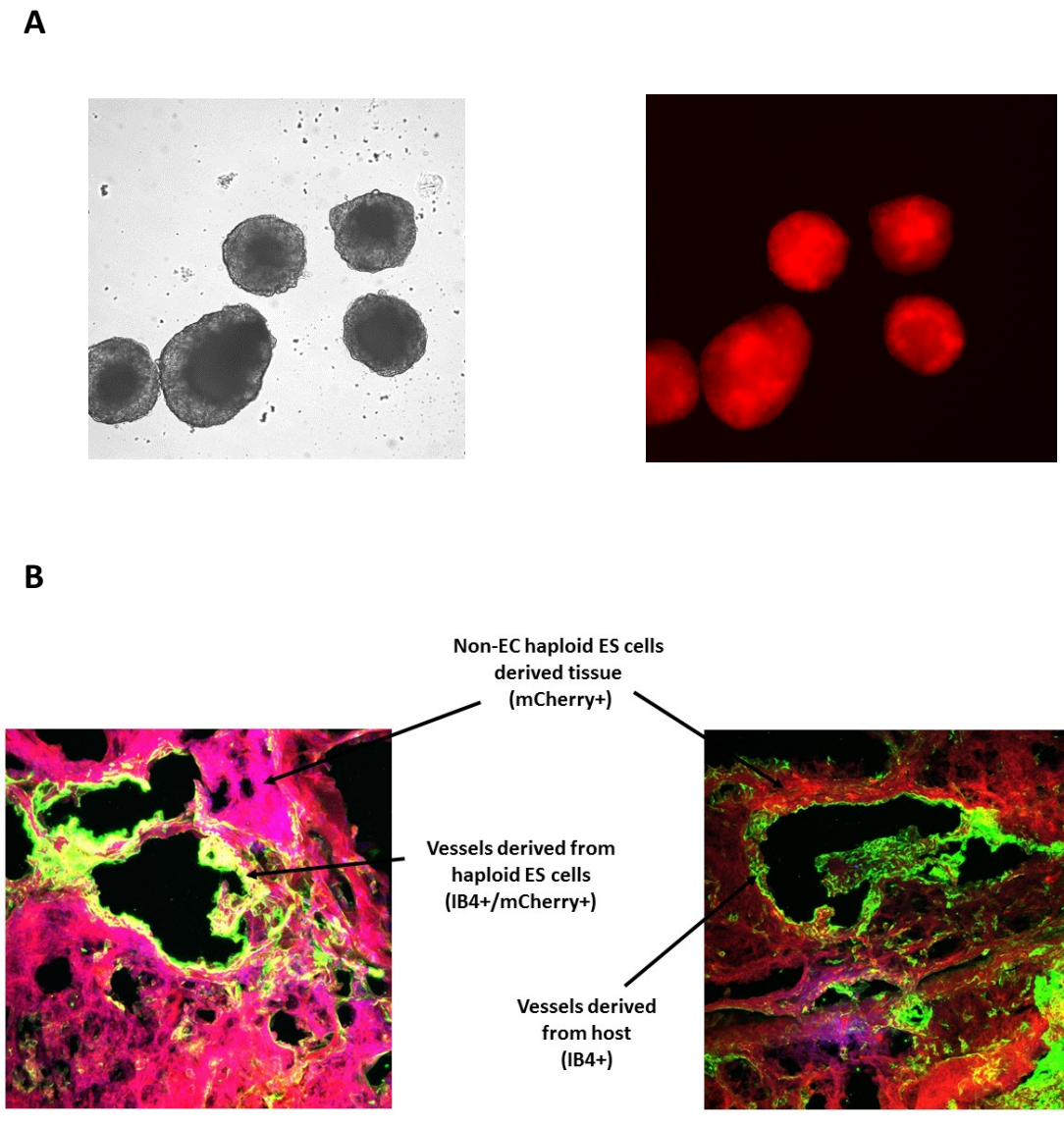

Figure 2.11 Formation of haploid ES cell-derived vasculature *in vivo.*
A m-Cherry-marked haploid EBs were used for *in vivo* injection into immunocompromised mice. **B** Haploid ES cell-derived teratomas were stained with IB4 to assess vascular composition. Vessels derived from host are shown in green ($IB4^+$) and haploid ES cell-derived vessels are shown in yellow ($IB4^+$ and m-$Cherry^+$). Non-EC tissues derived from haploid ES cells are shown in red (m-$Cherry^+$).

2.7 *In vivo* sprouting capacities of wildtype vs. mutated haploid ES cells

To evaluate the ability of our candidate clones to contribute to teratoma vasculature *in vivo*, we applied our EB injection assay on selected gene trapped clones that showed a noticeable hypersprouting or hyposprouting phenotype in the 3D collagen matrix assay. Those clones were the 3 hyposprouters; *Myst3*, *Gja1* and *Grin2b* and the 3 hypersprouters; *Enpp3*, *Plcb1* and *Ndufs4*. To ensure getting direct and unbiased comparable results for the assessment of wildtype v. mutant clones in terms of sprouting capacities, we generated EBs containing equal amounts of mutant and repaired (wildtype) cells of chosen haploid sister ES cell clones and injected them into immunocompromised mice. Notably, I performed this by either generating EBs initially made of equal amounts of wildtype and mutant cells which resulted in chimeric EBs that had both the GFP^+ and the M-$Cherry^+$ signals, or by generating two separate EB sets composed of wildtype or mutant EBs that were ultimately mixed for further injection.

Harvested teratomas were assayed in two ways; 1. *in situ* examination of cryosectioned EC-marked specimens, and 2. Analysing teratoma tissues by cytometry. Based on *in situ* examination, we could infer that teratoma vasculature was mainly composed of mouse cells. That was evident from regions shown to be positive for the IB4-EC marker while negative for both green and red signals derived from injected EBs. Nevertheless, we could reliably identify regions positive for both ECs and ES cell markers; inferred from their red or green fluorescent signals. These represented vessels derived from the injected ES cells. As we always examined sister clones comprising hyper or hypo-sprouting mutants along with their wildtype counterparts, we were particularly interested in exploring their relative contribution to ES cells derived vessels to assess how their *in vivo* sprouting behaviour matched their *in vitro* sprouting profile. Hypersprouting clones were more likely to contribute to vasculature compared to their wildtype counterparts. By contrast, wildtype sister clones of hyposprouting mutants showed more contribution to haploid ES cell-derived vessels compared to their mutant counterparts. Figure 2.12 shows a representative example of the hyposprouting *Gja1* clone.

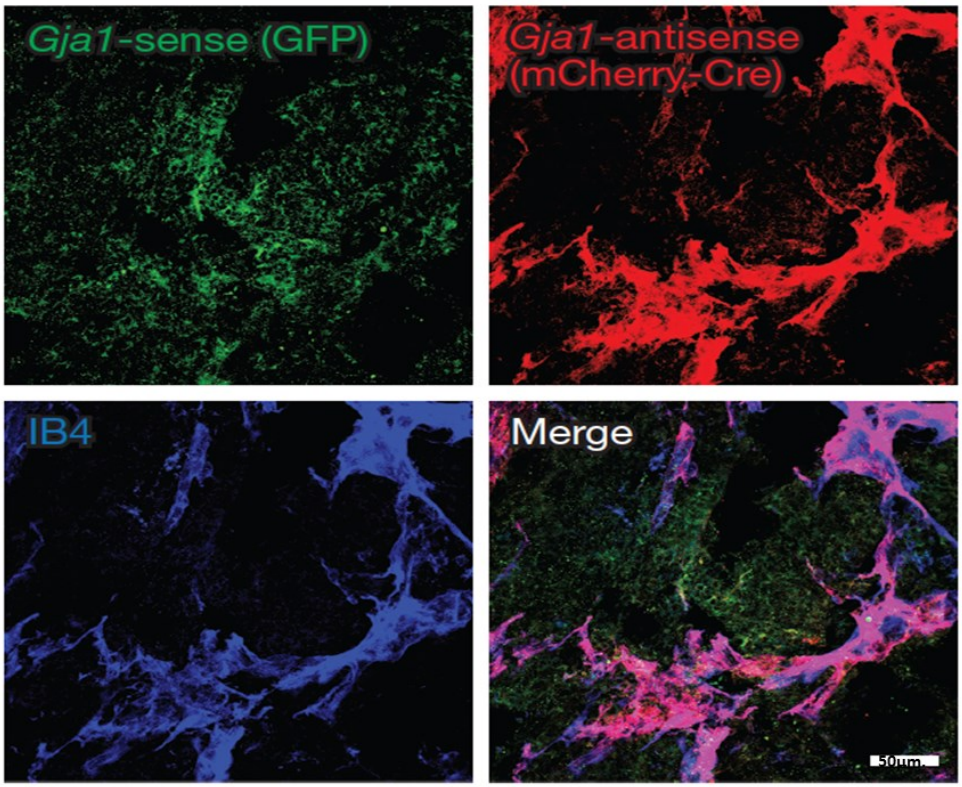

Figure 2.12 A representative example of *in vivo* blood vessel competition assay shown for the *Gja1* candidate gene.
Chimeric EBs were generated using a 1:1 ratio of both mutant (sense) and wildtype (antisense) *Gja1* haploid ES cells. EBs were subsequently injected subcutaneously into immunocompromised mice. By examining teratoma sections, the majority of ES cell-derived vessels originated from the wildtype *Gja1* clone inferred by an apparent co-localization between IB4^{+} (representing teratoma vessels) and m-Cherry+ cells (representing *Gja1* wildtype). On the contrary, *Gja1* mutant ES cells (marked by GFP^{+}) apparently lacked the ability to contribute to teratoma vasculature. Scale bar 50µm.

In order to quantify these results, we further analysed teratomas by FACS. To reliably evaluate the contribution of mutant vs. wildtype clones to the vasculature, we needed first to exclude general effects such as growth advantage/disadvantage or changes in overall differentiation. Therefore, we measured the differential contribution of sister clones for both, IB4 positive (EC) and IB4 negative (non-EC) lineages. Our results measuring GFP and m-Cherry fluorescent signals indicated that gene trapped clones and their wildtype counterparts contributed equally to the non-EC-cluster of analysed teratomas (Figure 2.13). This confirmed that the difference in sprouting profiles between sister-clones was the determining factor underlying their relative contribution to teratoma vessels. By analysing the endothelial fraction, our FACS results again

showed that hypersprouting mutants show more contribution to vasculature compared to wildtype sister clones, whereas hyposprouting mutants exhibit a lesser contribution in comparison to their corresponding wildtype sister clones (Figure 2.13).

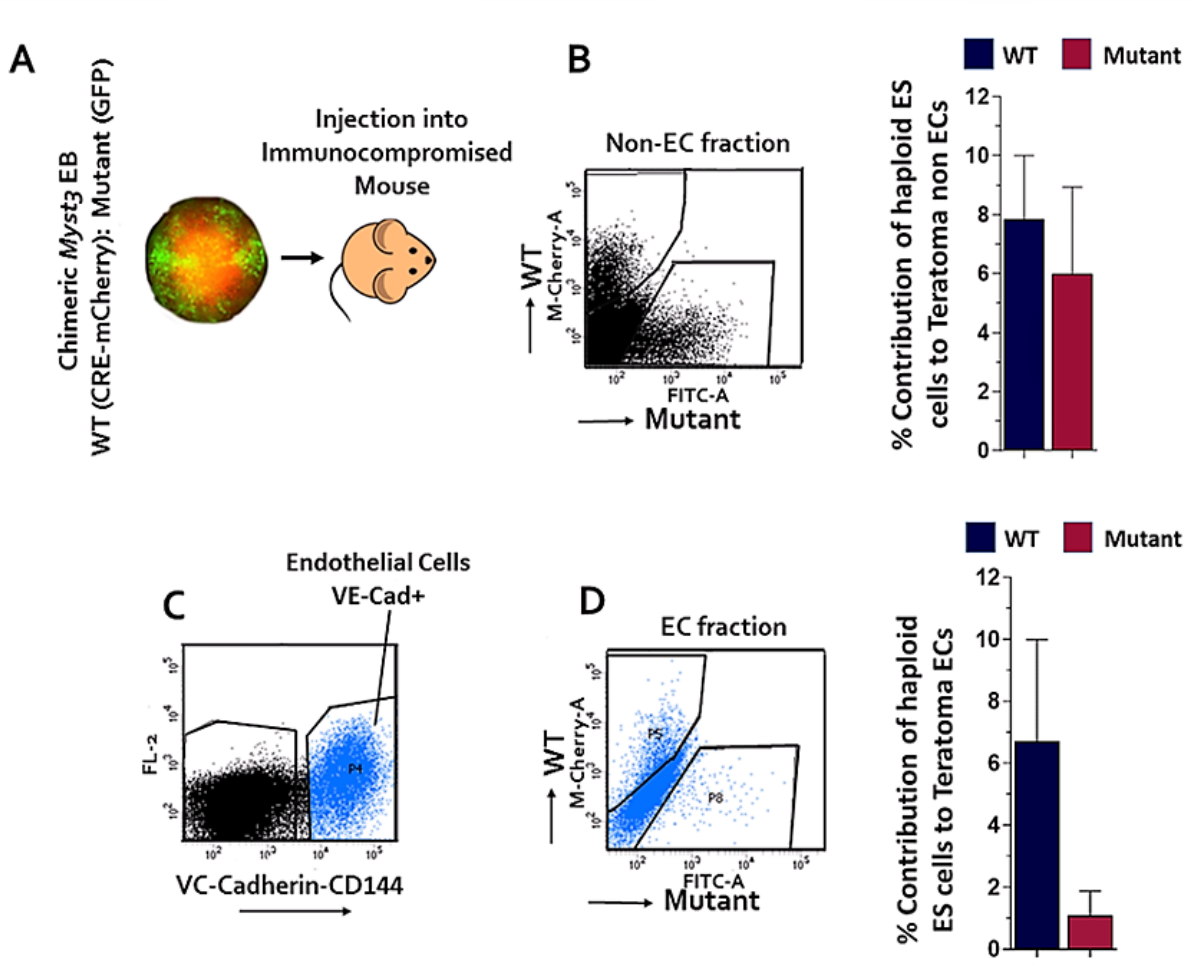

Figure 2.13 A representative FACS analysis of teratomas originating from wildtype/mutant *Myst3* chimeric EBs mixed in a 1:1 ratio.
A A scheme of the experiment set up: EBs were generated of WT and mutant *Myst3* sister clones mixed at a 1:1 ratio. EBs were subsequently injected in immunocompromised mice. **B** Contribution of injected haploid ES cells to the non-EC fraction of teratomas was assessed. Wildtype and mutant *Myst3* clones did not show an apparent difference in their contribution to the non-EC fraction. **C** VE-Cadherin (CD144) was used to mark the population of ECs. **D** wildtype *Myst3* clones contributed significantly more to teratoma vessels compared to the mutated counterparts which exhibited a dramatic decline in their ability to form vessels in the teratomas.

In conclusion, results obtained from analysing teratomas obtained from injecting EBs of the candidate genes *Myst3*, *Gja1* and *Grin2b,* previously identified as positive regulators for sprouting angiogenesis *in vitro,* confirmed that they were also required for blood

vessel formation *in vivo* as gene trapping led to their reduced contribution to the endothelial lineage. In contrast, *Enpp3*, *Plcb1* and *Ndufs4* that we identified as negative regulators of angiogenesis *in vitro* contributed more to the vascular lineage upon *in vivo* disruption of gene function (Figure 2.14)

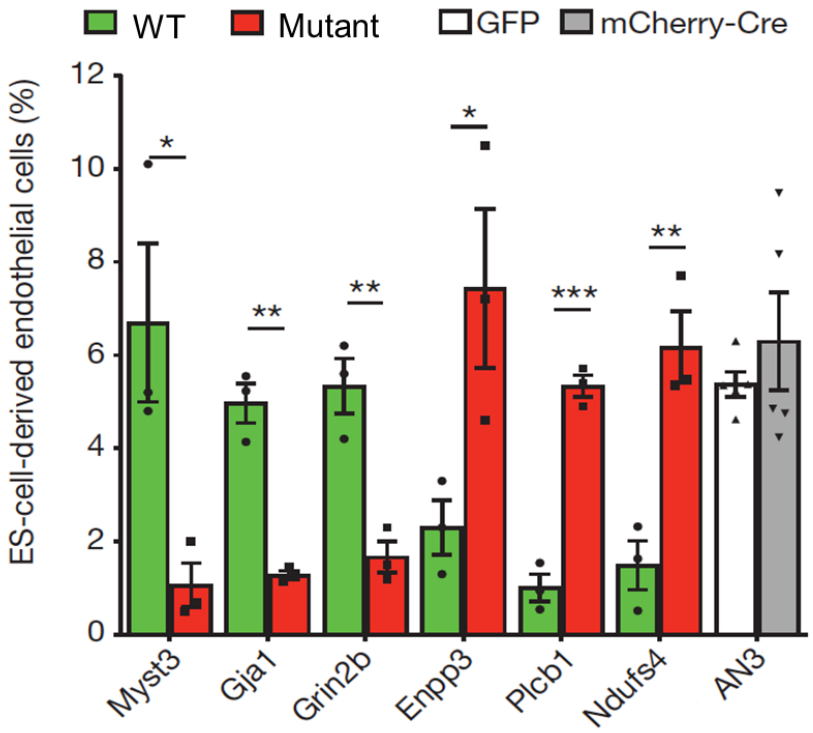

Figure 2.14 Contribution of wildtype and mutant clones of selected candidate genes to teratoma blood vessels.
Myst3, *Gja1* and *Grin2b* mutant ES cells exhibited a significantly reduced ability to contribute to teratoma vasculature compared to their wildtype sister clones while the mutated forms of *Enpp3*, *Plcb1* and *Ndufs4* showed a significant higher contribution to vessels compared to wildtypes. Data are mean values ± SEM. n=3-5 independent teratomas. * $P < 0.05$; ** $P < 0.01$; *** $P < 0.001$ (Students t-test). The contribution of GFP^+ /CRE m-$Cherry^+$ AN3 haploid ES cells to teratoma vasculature was assayed as control.

3 Discussion

Many *in vitro*, *ex vivo*, and *in vivo* assays and models have been developed and adopted in order to enable a better understanding of the basis and mechanisms by which new blood vessels form and perform (Cimpean et al. 2011). Nevertheless, comprehensive understanding of all the processes and pathways involved in angiogenesis has not yet been achieved. Many research projects focusing on angiogenesis are based on disrupting certain genes and studying the effect of this on vessel formation and phenotype. Contrary to the state of haploidy found in yeast, diploidy in somatic mammalian cells obscures recessive mutations where a second normal gene copy compensates for the mutated version found in the wildtype partner allele (Elling et al. 2011).

To overcome this, gene targeting by homologous recombination has been widely used to disrupt murine genes. In this context, the international project named the international knockout mouse consortium which aimed at creating mouse ES cells with a null mutation in every gene, has already covered most of the mouse genome (Bouabe, Okkenhaug 2013). Other approaches such as siRNA, shRNA or CRISPR also provide an efficient and useful tool to relate resulting phenotypes to the loss of function of certain genes (Elling et al. 2017). On the other hand, the generation of murine haploid ES cells has led to the consequent establishment of Haplobank as a source to provide researchers with murine ES cells that harbour homozygous gene mutations (Elling et al. 2011). This resource provides a very efficient and reliable way to enable a direct, unbiased and highly cost-effective tool for functional genetics studies. This is due to the advantage of reversibility of gene trap inserts which allows for the generation of repairable clones mediated by CRE recombinase. The advantage of this feature is embodied in the exclusion of clonal differences when the effect of mutating a certain gene is being assessed. This ensures that the observed phenotype in a mutated clone is due to the mere effect of losing gene function (Elling et al. 2017).

We utilized this system which combines the advantage of haploid genetics with the capacity of ES cells to differentiate into virtually all cell types of the body to discover novel regulators of angiogenesis. We generated repaired sister clones for each mutated candidate clone to exclude clonal variability and assess angiogenic sprouting behaviour in a 3D model of differentiation. As for the candidate clones, we chose our genes based on their differential expression in tip cells (del Toro et al. 2010; Strasser et al. 2010). The importance of studying such genes lies in the indispensable role of tip cells in driving and controlling the angiogenic process (Siemerink et al. 2013). Therefore, we thought that focusing on genes highly expressed in tip cells by directly studying the effect of disrupting them on the endogenous ability of cells to undergo angiogenesis might shed light on novel angiogenic regulatory players. We could in deed identify a tip cell phenotype in our tip cell competition assays which included hypersprouting or hyposprouting clones.

From the therapeutic aspect of view, tip cells are potentially an optimal target of study because of their direct role in inducing angiogenesis. Therefore, targeting tip cells could in principle abolish the angiogenic behaviour specially in pathological conditions where uncontrolled vessel growth leads to progression of the disease such as in cancer and ocular diseases (del Toro et al. 2010; Siemerink et al. 2013). This is particularly important since the main current treatment strategies interfere with normal blood vessel function which could result in serious side effect. For instance, Targeting VEGF using bevacizumab in combination with other therapeutic strategies like chemotherapy or radiation has been approved for several cancer types. In addition, a significant progress was made in treating ocular neovascularization using anti-VEGF drugs as well (Siemerink et al. 2013; Potente et al. 2011). However, one of the major debates against the anti-VEGF therapy is its possible adverse effects on normal vasculature where quiescent endothelial cells need continuous low levels of VEGF for their survival (Casanovas 2012). Therefore, specific targeting of tip cells without interfering with the quiescent endothelium would be an ideal alternative to the current treatment options (Siemerink et al. 2013). This could be achieved by identifying specific tip cell molecules found to have a regulatory role on angiogenesis and subsequently targeting them to either block uncontrolled

vessel growth or stimulate and guide vessel growth towards ischemic areas (del Toro et al. 2010; Siemerink et al. 2013). For this purpose, our candidate tip genes were also chosen based on their reported link to human vascular diseases.

Our results show the effect of disrupting the chosen genes on the angiogenic process. We could consequently identify novel regulators of angiogenesis, five that significantly increased sprouting (hypersprouters) and eight that significantly inhibited the sprouting process (hyposprouters). We could also demonstrate the importance of some of these regulators in an *in vivo* competition model. To be able to unveil the specific roles and/or the pathways that each of these gene candidates undergo with regard to angiogenesis, it is particularly important as a future approach to further study the interactions and the physiological roles that each of these genes play. For instance, the *Enpp3* gene encodes a type II transmembrane ectoenzyme that belongs to the ecto-nucleotide pyrophosphatases/phosphodiesterases family (ENPPs) which hydrolyse extracellular nucleotides and release nucleotide mono phosphates (Goding et al. 2003). ATP and adenosine in particular are among the most significant extracellular nucleotides involved in a wide range of biological responses that include regulation of cell proliferation and differentiation. ATP and adenosine exert their function by activating their purinergic receptors denoted P2 and P1, respectively. Hydrolysis of ATP by ENPPs activates P1 signalling on expense of signalling by the P2 receptor (Goding et al. 2003). To relate this to our results, it is conceivable that depriving cells of ENPP3 will favour ATP-mediated P2 signalling which in turn might have a stimulatory effect on angiogenesis represented by the observed increase in vessel formation.

Another possible assumption to explain the observed hypersprouting phenotype in *Enpp3* mutant clones is by shedding light on its inhibitory role on some molecules known to stimulate angiogenesis. A study performed by Korekane et al has revealed a regulatory role of ENPP3 for *G*nT-Vb (a closely related homolog of GnT-V) in Neuro2a (N2a) cells (Korekane et al. 2013). GnT-Vb is a brain-specific N-acetylglucosaminyltransferase whose inhibition by ENPP3 was shown to occur through hydrolysis of UDP-GlcNAc, a nucleotide sugar donor, to UMP which works as a potent

Gnt-Vb inhibitor (Korekane et al. 2013). Although the effect of ENPP3 on angiogenesis has not been previously elucidated to our knowledge, some studies on the other hand linked GnT-V to cancer angiogenesis. The secreted form of GnT-V was shown to promote angiogenesis by inducing the release of FGF2 and was proposed to play a role in tumor progression and metastasis (Nakahara et al. 2006; Saito et al. 2002). Since ENPP3 has been shown to exert an inhibitory effect on GnT-Vb, this coincides with the proposition that disrupting the *Ennp3* gene will abolish the inhibitory effect it exerts on its substrate (GnT-Vb) leading to enhanced vessel formation. It is therefore also possible that the observed increase in vessel formation in *Enpp3* gene trapped clone could be attributed to its negative effect on GnT-Vb. In general, we could speculate that ENPP3 could have a regulatory role in angiogenesis that might function through inhibiting certain glycosyltransferases such as GnT-Vb and/or others. Evidently, further studies are required to understand and explain the exact regulatory role of ENPP3 in vessel formation.

Gja1 is one of our eight hyposprouting gene candidate hits that included also *Myst3*, *Mecom*, *Gabrb3*, *Tnfrsf1a*, *Dlg2, Grin2b and Cdh13* clones. When mutated, *Gja1* exhibited a significant decline in the ES cells ability to form vessels and undergo angiogenesis in both collagen matrix assay and *in vivo* teratoma assay. *Gja1* encodes a gap junction protein called connexin 43 (Cx43) (Chen et al. 2015). Gap junctions are cell-cell interaction points where 2 hemichannels of each cell dock to form sites in the plasma membrane through which small molecules and ions can pass from one cell to another in a way that preserves homeostasis in an organism (Sohl, Willecke 2004; Bobbie et al. 2010). Cx43 is ubiquitously found in many cell types (Kameritsch et al. 2012). In the cardiovascular system, it is present along with other connexins (Cx37, Cx40 and Cx45) and has been shown to play a crucial role. Cx43 is expressed in cardiac muscle cells, smooth muscle cells of the vasculature as well as in endothelial cells. Endothelial cell specific Cx43 knockout was shown to cause hypotension and bradycardia in transgenic mice (Liao et al. 2001). Knocking out Cx43 was also shown to be lethal in neonatal mice and caused death due to heart failure. (Reaume et al. 1995).

Importantly, *Gja1* has been reportedly linked to cells migration and proliferation (Chen et al. 2015). However, controversy was reported pertaining the effect of Cx43 loss on cells ability to migrate and proliferate. In one hand, a proportional relationship was proposed between Cx43 levels and the migratory and proliferation behaviour of cells (Kameritsch et al. 2012). For example, high level of Cx43 was shown to be associated with migrating endothelial cells during the process of wound healing *in vivo*, a role that has been shown to be dependent on the presence of a functional carboxyl tail (Homkajorn et al. 2010). It was proposed that connexins play part of their role in this regard by allowing calcium ion flow and propagation between migrating cells through gap junctions. Hemichannels alone on the other hand were also shown to exert a related function by releasing ATP that induces calcium signalling in neighbouring cells (Homkajorn et al. 2010) . Apart from its classical channel-dependent role, accumulating data suggest that connexins can also exert some of their functions in a channel-independent manner. For instance, the carboxyl tail of Cx43 was shown to be independently capable of driving cell motility of human glioma cells (Crespin et al. 2010). Of note, the carboxyl tail of connexins being subject to phosphorylation by many kinases can bind to transcription factors and cytoskeleton proteins (Kameritsch et al. 2012).

Besides its role in cell migration, some studies aimed at exploring the effect of Cx43 depravation directly on the angiogenic process as well. For example, Wang et.al reported that silencing of Cx43 following siRNA transfection of endothelial progenitor cells (EPCs) resulted in a significant decline in the angiogenic potential observed using Matrigel assays taking into consideration that Cx43 is the main gap junction constituent in EPCs (Wang et al. 2013). Interestingly, it was further shown in this study that this angiogenic reduction ability was associated with reduced VEGF transcription levels and that the diminished angiogenic phenotype could not be compensated by externally providing VEGF to the cells. This correlation with VEGF production has been also reported in another study that linked the overexpression of Cx43 in mesenchymal stem cells with an increased secretion of VEGF and bFGF under hypoxic conditions where this effect has been shown to take place in a channel-independent manner as well (Wang et al. 2014).

Overall, the diminished angiogenic phenotype observed as a result of Cx43 silencing coincides with our results which demonstrated that Cx43 gene trapping resulted in a significant diminished sprouting capacity of ES cells both *in vitro* and *in vivo*. Conversely, some research studies proposed an inverse relationship between the levels of Cx43 and the cellular migration and proliferation behaviour. Among these, a 2015 study by Choudhary et. al. demonstrated that Cx43 heterozygous mice injected with mammary tumor cells showed a significant increase in tumor vasculature compared to control (Choudhary et al. 2015). It was also proposed that tumor cells induce angiogenesis by downregulating Cx43 which normally interacts with mural cells to keep endothelial quiescence (Choudhary et al. 2015). This effect was explained by an established association between mural and endothelial cells where heterologous gap junctions are shared between the two types of cells. This association was shown to be diminished when exposed to breast tumor media which liberates ECs and exposes them to the surrounding angiogenic cues (Choudhary et al. 2015). This corresponds to the features of tumor vasculature characterized by having a declined and disorganized connection to mural cells which renders the vessels leaky and fragile (Fouad, Aanei 2017). The controversy presented regarding Cx43 might be attributed to differences in the physiological role of Cx43 in normal and tumor cells. Therefore, it could be hypothesized that in normal vessels where the association between mural and endothelial cells is preserved and tightly controlled, Cx43 exerts its role in facilitating new vessel formation in a well-organized and controlled manner by the above discussed channel dependent and independent roles. This may explain why reduction of Cx43 causes a diminished ability of vessels to grow, as seen in our ES cells. On the other hand, the effect of reduced Cx43 levels in the tumor vasculature might favour tumorigenesis by diminishing mural-EC connections, therefore overriding the negative effect of Cx43 reduction on angiogenesis seen in normal cells.

4 Materials and Methods

4.1 Haploid embryonic stem cell culture

Haploid ES cells were grown using a standard ES cell medium (ESCM). This was prepared using 408.85ml DMEM (Sigma D1152), 75ml FCS (10%, Invitrogen), 5ml Pen/ Strep (Sigma P0781), 5ml L-Glu (Sigma G7513), 5ml non-essential. amino acids (Sigma M7145), 5ml Sodium Pyruvate (Sigma S8636), 550µl β-Mercaptoethanol (Merck, 805740, 10µl βME was diluted in 2.85ml PBS for 1,000X stock), and 5µl Leukaemia inhibitory factor (LIF). For the selection medium, puromycin 10µg/mL (Invitrogen) was added.

For cultivation of haploid ES cells, we used cell culture treated dishes as follows: from Greiner; 15cm dishes (15cm CellStar cell culture dishes, cat no 639160). And from NUNC; (10cm dishes, Nunclon Δ Surface, cat no. 150350, and 6-well Nunclon Δ Surface, cat no. 140675). Haploid ES cells of all the clones of interest were thawed by adding 5ml of warm selective ESCM, and then centrifuged at 1000 rpm for 5min to remove of the freezing medium. Pellets were resuspended in ESCM and plated under feeder free conditions on 10cm dishes. For freezing, haploid ES cell clones from each candidate clone were expanded in 10cm dishes till they reached confluency, then trypsinized at 37°C for 5min. Cells were resuspended in selective ESCM to stop the reaction and were then centrifuged at 1000rpm for 5min. After discarding supernatants, pellets were resuspended in 7ml sterile-filtered freezing medium (50% FBS, 40% ESCM with puromycin, 10% DMSO (Sigma# 41648)) and distributed into 4X 2ml labelled cryovials that were subsequently stored at -80°C.

4.2 Barcode PCR and Sanger sequencing for confirmation of haploid ES cell clone identities

$1X10^6$ cells of each haploid ES cell candidate clone were harvested and centrifuged at 1000rpm for 5 minutes. Supernatants were discarded and pellets resuspended in 45µl lysis buffer (100mM Tris-HCl; pH 8.5, 5mM EDTA, 0.2% SDS, 200mM NaCl) + 5µl Proteinase K (1mg/ml) and incubated overnight at 55°C. Proteinase K was then deactivated by incubating samples at 95°C for 10min. For each DNA sample, a mixture of 400µl absolute ethanol and 6µl 5M NaCl was added and samples were kept on ice for 20 min until DNA threads formed. Samples were centrifuged at 4500 rpm for 30min at 4°C and supernatants were discarded. DNA pellets were washed once with 400µl absolute ethanol and centrifuged again at 4500 rpm for 20min at 4°C. Supernatants were discarded and DNA pellets were left to dry at RT for 2-3min. DNA pellets were finally resolved in 100µl 1X TE for 90min at 55°C and later stored at 4°C.

Barcode PCR reaction

gDNA 100ng/µl	2µl
Primer barcode PCR-Forward 100µM	0.1µl
Primer barcode PCR-Reverse 100µM	0.1µl
10mM dNTP mix	1µl
10x Encyclo buffer	5µl
50x Encyclo polymerase	1µl
dH2O	40.8µl

Primer barcode PCR-Forward sequence:
GGTTGATCTGAGCTACTCATCAACGGT

Primer barcode PCR-Reverse sequence:
CAAGTTCCTTCTGGTTCTGGCTCTGCT

Biorad C1000 cycle parameters:

95deg, 3’

95deg, 10” |

58deg, 20” | 32x

72deg, 30” |

72deg, 5’

From the total of the 50µl PCR reaction, 20µl were used for electrophoretic separation on a 2% agarose gel. The remaining PCR reaction was used for Sanger sequencing using 5µl PCR reaction and 2µl illustra ExoStar 1 – step kit (GE Healthcare). The mixture was run in thermal cycler for 15min at 37°C and then for 15min at 80°C. 3µl of the prepared DNA was then used for sequencing by adding 0.3µl barcode PCR-reverse primer and ddH2O to fill a total of 7µl.

4.3 Haploid ES cells infected with GFP and CRE m-Cherry fluorescent constructs

4.3.1 Transformation of bacterial cells and DNA plasmid preparation

50-100µl competent cells (DH5-Alpha) were thawed slowly on ice and then incubated with 0.5µl plasmid DNA (GFP or CRE m-Cherry or gag-pol) for 40min on ice. Cells were then heat-shocked by placing the tubes in a water bath at 42°C for 45sec following incubating them for 2min on ice. 1ml prewarmed LB medium was then added and bacteria were grown for 1h in a 37°C shaking incubator. Transformed cells were then centrifuged at 10000g for 1min and resuspended in 100µl LB medium. The bacteria were plated onto an Ampicillin selective 10cm LB agar plate and incubated overnight at 37°C. Transformed bacterial colonies were picked and inoculated into 2ml ampicillin selective LB medium and grown for 2h in a 37°C shaking incubator. Subsequently, the bacterial preculture was added into 200ml ampicillin selective LB medium and incubated

overnight at 37°C in a shaking incubator. Bacterial cells were then centrifuged at 6000g for 15 min and pellets were used to purify the respective plasmids using QIAGEN Plasmid Maxi Kit (QIAGEN Cat No./ID: 12163) following the manufacturer protocol.

4.3.2 Plat-E cells transfection

Haploid ES cell clones were infected by ecotropic retroviruses containing either GFP - puro or CRE m-Cherry – puro constructs. Retrovirus production was achieved by the transfection of packaging cells as follows:

For transfection of a 10-cm plate of packaging cells:

Solution A (500µl): 20µg DNA Plasmids containing GFP or CRE m-Cherry constructs with a puromycin selective marker, 10µg Helper DNA (pCMV-Gag-Pol), H_2O (437.5µl – vol. of added DNA), 62.5 µl 2M $CaCl_2$.

Solution B (500 µl): 2X HBS.

2X HBS (HEPES-Buffered Saline) 1000µl was made as follows: 280 mM NaCl, 50 mM HEPES, 1.5 mM Na_2HPO_4, 12 mM Dextrose, 10 mM KCl, 1000µl H_2O. pH was adjusted to be between 6.96-7.08.

Before use, all prepared solutions were sterile-filtered using 0.2µl filters. If were not used directly, filtered solutions were kept in 10ml aliquots and stored at -20°C.

The Platinum-E (Plat-E) retroviral packaging cell line (Cell Biolabs) was used for transfection. Plat-E cells were cultivated using a standard medium: 408.85ml DMEM, 50ml FBS 10% (Invitrogen), 5ml Pen/ Strep (100 U Pen/ml; 0.1mg Strep/ml (Sigma). After reaching 75 - 85% confluency, transfection of plat-E cells was performed as follows: Solution A was added drop-wise to solution B while using a pipet-aid to blow bubbles in solution B. The turbid mixture was left at RT for 15min before being added drop wise to the packaging cells. After 24h of transfection, standard medium was exchanged with ESCM. After 36h of transfection, retroviruses were collected every 6 hours, filtered

through a 0.45µl filter and stored at -80°C for subsequent infection of haploid ESC clones.

4.3.3 Infection of haploid ES cells

Haploid ES cells were thawed and cultured using ESCM in 6-well plates. 6 candidates carrying integrations in genes were dealt with at a time such that each clone was occupying 2 vertical wells. Each well contained 1 x 10^5 cells. Each candidate clone was infected by retroviruses containing either GFP or CRE m-Cherry as follows: Medium was removed, 1ml pre-prepared GFP or CRE m-Cherry expressing retroviral solution was added on top of the cultured haploid ES cells and incubated for 2-3h at 37°C. 2ml of ESCM were then added and the medium was exchanged after 24h. 48 hours after infection, ESCM was replaced by selective medium (ESCM+ puromycin (10 µg/mL).

4.3.4 FACS Sorting of fluorescent ES Cells

48h after infection with GFP or CRE m-Cherry, haploid ES cells carrying retroviruses were sorted for fluorescent cells: Once cells reached confluency, they were trypsinized, and sorted by fluorescence-activated cell sorting (FACS) using a BD FACS Aria III, such that the highest 5% fluorescent cells were obtained separately. This portion of cells, usually comprising 100,000 – 150,000 GFP or CRE m-Cherry expressing cells, was cultivated using selective ESCM and subsequently used to make EBs for *in vitro* and *in vivo* studies.

4.4 Haploid ES cell *in vitro* sprouting model

4.4.1 EB formation and vascular differentiation

Wildtype haploid ES cells (gene trap in antisense) and their mutagenized counterparts (gene trap in sense) were used to make blood vessel organoids as follows: GFP and CRE m-Cherry marked haploid ES cells were trypsinized and 9600 cells from each were seeded in 96-well low attachment plates (Sumitomo Bakelite, Prime Surface-U) to allow

EB formation. Media used for EBs was ESCM without LIF to allow cell differentiation and formation of EBs. EBs were washed using EB medium (ESCM -LIF) once during the process of EB formation. After an incubation period of around 8 days, EBs were washed and added to 6-well plates containing a pre-added and solidified first layer of collagen matrix on an average of 6-8 EBs/well. A second layer of freshly prepared collagen was then added over the EBs which were then distributed spatially throughout the plate. The Collagen matrix was then left to solidify by incubation for 2h. 50ng/ml VEGF-A (in house)-containing EB medium was then added on top of the collagen gel to stimulate vascular growth. After incubation for about 10 days, the sprouting capacities of EBs of the various candidate clones were initially evaluated by visualizing the sprouts under a brightfield microscope.

The Tip cell competition assay was performed by generating 1:1 mixed EBs generated from both GFP and CRE m-Cherry infected haploid ES cells. The same procedure was followed to generate and embed the mixed EBs in collagen matrix. However, a selective EB medium containing (1:10000) puromycin was used for the competition assay instead. Sprouts generated from mixed EBs were visualized using a Zeiss LSM780 scanning confocal microscope to evaluate tip cell dominancy.

Collagen matrix composition:

	Volume in mL
NaOH 0.1N	$6.25 * 10^{-2}$
10xDMEM	$6.25 * 10^{-2}$
Hepes	$1.25 * 10^{-2}$
Bicarb	$9.77 * 10^{-3}$
Glutamax	$6.25 * 10^{-3}$
1xF12	$3.46 * 10^{-1}$
Collagen	$5 * 10^{-1}$
Tot. vol.:	1

Two layers of collagen were added such that the first layer constituted 600µl/well and the second layer constituted 700µl/well.

4.4.2 Imaging of EB sprouts

Sprouted EBs were prepared for microscopic visualization as follows: Medium was aspirated and sprouts were fixed using 4% paraformaldehyde (PFA) in PBS for 15min at RT. Gels were liberated from the wells by using forceps and were then transferred to PBS filled petri dishes. Empty gel edges were discarded using a scalpel and a chosen portion that contains 3-4 sprouting EBs was cut for staining while the rest was kept for future use. The two gel layers were separated with the aid of sharp forceps and then transferred to 2ml tubes. The gel was permeabilized and blocked in blocking buffer consisting of 3% FBS (Gibco), 1% BSA (AppliChem), 0.5%Triton (Sigma), 0.5% Tween (Sigma) and 1% Na deoxycholate (Sigma) added for 2h at RT on a rocking platform. For staining of endothelial cells, biotinylated Isolectin B4 (IB4; Vectorlabs 1201) and anti-CD31 (BD Pharmingen AB9498; 1:50) primary antibodies in blocking buffer were applied over night at 4°C on a rocking platform. Gels were then washed 3-4 times using PBS-T (Tween 0.05%), 10-15min/wash. Streptavidin-Alexa488 (1:500) and anti-rat-Alexa488 fluorescent secondary antibodies (1:500) in blocking buffer were then added to the gels and kept for 2h at RT followed by washing 3-4 times in PBS-T. Nuclear labelling was performed using DAPI (1:1000) solution followed by a final washing with PBS-T. With the aid of a stereomicroscope, gels containing the stained sprouts were mounted on slides using DAKO mounting medium, covered with coverslips and labelled. Vascular outgrowth of each candidate clone was then visualized by a Zeiss LSM780 scanning confocal microscope using tile scanning and z-stacks options. Analysis of the obtained pictures was performed using the Image-J software.

4.5 *In vivo* sprouting model

4.5.1 Teratoma assays

Wildtype/Mutant EBs (1:1 mix) were used for the generation of chimeric vasculature *in vivo as* follows: A total of $2X10^6$ haploid ES cells containing equal numbers of both GFP and CRE m-Cherry infected cells were cultured in 15cm Petri dishes to generate chimeric

EBs. Alternatively, $1X10^6$ haploid ES cells of each GFP or CRE m-Cherry clones were cultured separately in 15cm petri dishes and were ultimately mixed before injection (mixed EBs). EBs formed by either setup were cultured under puromycin selection pressure to avert possible reporter silencing. After 8 days in culture, EBs were washed and resuspended in 200ml growth factor-reduced Matrigel (BD 356231). EBs-contained Matrigel was kept on ice to slow down the process of Matrigel hardening. EBs were subsequently injected subcutaneously into the right and left sides of 8-12-week-old female and male immunocompromised MF1 *nu/nu* mice with the aid of a 18G needle and grown teratomas were harvested and analysed 3-4 weeks after EBs injection.

All mouse experimental studies were approved in accordance with the Austrian and EU legislature

4.5.2 Teratoma Analysis

Harvested teratomas were processed in two ways: Half of the obtained teratoma was used for FACS analysis, and the other half was used for immunohistochemistry.

For FACS analysis, tissues were placed on petri dishes, and minced using scissors. Subsequently, enzymatic digestion was performed using 0.2 sterile filtered Collagenase IV buffer solution consisting of Collagenase Type IV 300U/mL (Worthingtion), Dispase 0.25U/mL (Gibco) and DNAse 7.5ug/mL (Quiagen). 1g of tissue of each teratoma was resolved in 10 ml of Collagenase IV buffer in 15ml tubes and kept for 45-60min at RT on a rocking platform while pipetting every 10 minutes for proper enzymatic digestion. Suspended cells were then pipetted through a 70µm cell strainer into 50ml tubes and passed through the sieve by compressing with a plunger from a 1ml syringe. The cell strainer was washed with DMEM and the cell suspension subsequently centrifuged at 400g for 10min. After washing the cell pellets once in DMEM, supernatants were discarded and pellets resuspended in 1ml FACS medium (RPMI (Gibco), 0.1 % BSA (Sigma). Cells were then counted using a CASY cell counter and distributed into 1.5ml Eppendorf tubes such that each vial contained $2X10^6$ cells. 200µl cells of each sample

was taken as a negative control. Non-specific binding of subsequent immunofluorescent staining was prevented by adding (1:200) mouse Fc block (anti CD16/32, BD 553142) (for 5-10min on ice. Anti-mouse VE-Cadherin-APC primary antibody (CD144) (ebioscience 17-1441-80) (1:100) was added to the cells which were then incubated for 45min on ice. Nuclear staining for dead cells was performed using DAPI (1:1000) for 5min to exclude dead cells from FACS analysis. Cells were then washed in FACS medium 3 times and a final 500µl FACS medium was added. Samples were subsequently transferred to FACS tubes and cell analysis was achieved using a FACS BD LSRFortessa (BD Biosciences).

For immunohistochemistry, Teratomas were fixed using 4% PFA over-night at 4°C, and subsequently incubated in 20%sucrose for around 24 hours before embedding into O.C.T. Fixed tissues were then embedded in cubes containing O.C.T freezing medium placed on dry ice to accelerate solidification. Labelled samples were either kept at this stage in -80°C or processed directly. 40-80mm thick sections were then cut from the teratomas using a cryostat and placed on glass slides kept in -20°C for subsequent immunostaining. Sections were dried for 10-20 at RT, then by using a liquid blocker pen, tissues were encircled and fixed using 300µL 4% PFA added to the confined area for 1h in a wet chamber to avoid drying out of the samples. Tissues were then washed 3X with PBS and embedded in protease type XIV (from Streptomyces griseus, Sigma) for 8min to enhance immunostaining intensity. 3X washes with PBS were then performed and tissues blocked with 1% BSA for 30min. Samples were subsequently incubated with primary antibodies (1:50) as follows: biotinylated-IB4 (Vectorlabs, #1201), anti-GFP (Abcam, AB111258) and anti-m-Cherry (Abcam, AB125096) overnight at 4°C. Sections were washed 3X with PBS and incubated with streptavidin-Alexa633, anti-goat-Alexa488, anti-mouse-Alexa555 secondary antibodies (1:500) for 1h at RT. Samples were washed 3X with PBS and incubated with DAPI (1:3000) for 10min. Finally, sections were washed 2X with PBS and mounted with DAKO mounting medium. Once dried, mounted samples were stored at 4°C until visualized. Imaging of teratoma specimens was performed using a Zeiss LSM780 scanning confocal microscope.

Publication bibliography

Adams, Ralf H.; Eichmann, Anne (2010): Axon guidance molecules in vascular patterning. In *Cold Spring Harb Perspect Biol* 2 (5), a001875. DOI: 10.1101/cshperspect.a001875.

Aird, William C. (2012): Endothelial cell heterogeneity. In *Cold Spring Harb Perspect Med* 2 (1), a006429. DOI: 10.1101/cshperspect.a006429.

Barry, Isobel (2008): Angiogenesis. VEGFR3 joins the crew. In *Nat Rev Cancer* 8 (9), pp. 660–661. DOI: 10.1038/nrc2446.

Benedito, Rui; Roca, Cristina; Sörensen, Inga; Adams, Susanne; Gossler, Achim; Fruttiger, Marcus; Adams, Ralf H. (2009): The notch ligands Dll4 and Jagged1 have opposing effects on angiogenesis. In *Cell* 137 (6), pp. 1124–1135. DOI: 10.1016/j.cell.2009.03.025.

Bentley, Katie; Mariggi, Giovanni; Gerhardt, Holger; Bates, Paul A. (2009): Tipping the balance: robustness of tip cell selection, migration and fusion in angiogenesis. In *PLoS computational biology* 5 (10), e1000549. DOI: 10.1371/journal.pcbi.1000549.

Blanco, Raquel; Gerhardt, Holger (2013): VEGF and Notch in tip and stalk cell selection. In *Cold Spring Harbor perspectives in medicine* 3 (1), a006569. DOI: 10.1101/cshperspect.a006569.

Boareto, Marcelo; Jolly, Mohit Kumar; Ben-Jacob, Eshel; Onuchic, José N. (2015): Jagged mediates differences in normal and tumor angiogenesis by affecting tip-stalk fate decision. In *Proc Natl Acad Sci USA* 112 (29), E3836-E3844. DOI: 10.1073/pnas.1511814112.

Bobbie, Michael W.; Roy, Sumon; Trudeau, Kyle; Munger, Stephanie J.; Simon, Alexander M.; Roy, Sayon (2010): Reduced connexin 43 expression and its effect on the development of vascular lesions in retinas of diabetic mice. In *Investigative ophthalmology & visual science* 51 (7), pp. 3758–3763. DOI: 10.1167/iovs.09-4489.

Bochenek, Magdalena L.; Dickinson, Sarah; Astin, Jonathan W.; Adams, Ralf H.; Nobes, Catherine D. (2010): Ephrin-B2 regulates endothelial cell morphology and motility independently of Eph-receptor binding. In *J. Cell. Sci.* 123 (Pt 8), pp. 1235–1246. DOI: 10.1242/jcs.061903.

Bouabe, Hicham; Okkenhaug, Klaus (2013): Gene targeting in mice. A review. In *Methods in molecular biology (Clifton, N.J.)* 1064, pp. 315–336. DOI: 10.1007/978-1-62703-601-6_23.

Bouïs, D.; Hospers, G. A.; Meijer, C.; Molema, G.; Mulder, N. H. (2001): Endothelium in vitro: a review of human vascular endothelial cell lines for blood vessel-related research. In *Angiogenesis* 4 (2), pp. 91–102.

Brudno, Yevgeny; Ennett-Shepard, Alessandra B.; Chen, Ruth R.; Aizenberg, Michael; Mooney, David J. (2013): Enhancing microvascular formation and vessel maturation through temporal control over multiple pro-angiogenic and pro-maturation factors. In *Biomaterials* 34 (36), pp. 9201–9209. DOI: 10.1016/j.biomaterials.2013.08.007.

Bulic-Jakus, Floriana; Ulamec, Monika; Vlahovic, Maja; Sincic, Nino; Katusic, Ana; Juric-Lekc, Gordana et al. (2006): Of mice and men: teratomas and teratocarcinomas. In *Collegium antropologicum* 30 (4), pp. 921–924.

Carmeliet, P. (1996): Abnormal blood vessel development and lethality in embryos lacking a single VEGF allele. In *Nature* 380, pp. 435–439.

Carmeliet, Peter; Jain, Rakesh K. (2011a): Molecular mechanisms and clinical applications of angiogenesis. In *Nature* 473 (7347), pp. 298–307. DOI: 10.1038/nature10144.

Carmeliet, Peter; Jain, Rakesh K. (2011b): Principles and mechanisms of vessel normalization for cancer and other angiogenic diseases. In *Nature reviews. Drug discovery* 10 (6), pp. 417–427. DOI: 10.1038/nrd3455.

Carmeliet Peter (2000): Angiogenesis in cancer and other diseases. In *Nature*.

Casanovas, Oriol (2012): Cancer. Limitations of therapies exposed. In *Nature* 484 (7392), pp. 44–46. DOI: 10.1038/484044a.

Chen, Cheng-Hung; Mayo, Jamie N.; Gourdie, Robert G.; Johnstone, Scott R.; Isakson, Brant E.; Bearden, Shawn E. (2015): The connexin 43/ZO-1 complex regulates cerebral endothelial F-actin architecture and migration. In *American journal of physiology. Cell physiology* 309 (9), C600-7. DOI: 10.1152/ajpcell.00155.2015.

Chen, Ying; Zhang, Yi; Deng, Qinyin; Shan, Nan; Peng, Wei; Luo, Xin et al. (2016): Inhibition of Wnt Inhibitory Factor 1 Under Hypoxic Condition in Human Umbilical Vein Endothelial Cells Promoted Angiogenesis in Vitro. In *Reproductive sciences (Thousand Oaks, Calif.)* 23 (10), pp. 1348–1358. DOI: 10.1177/1933719116638174.

Cherry, S. R.; Biniszkiewicz, D.; van Parijs, L.; Baltimore, D.; Jaenisch, R. (2000): Retroviral expression in embryonic stem cells and hematopoietic stem cells. In *Molecular and cellular biology* 20 (20), pp. 7419–7426.

Choudhary, Mayur; Naczki, Christine; Chen, Wenhong; Barlow, Keith D.; Case, L. Douglas; Metheny-Barlow, Linda J. (2015): Tumor-induced loss of mural Connexin 43 gap junction activity promotes endothelial proliferation. In *BMC cancer* 15, p. 427. DOI: 10.1186/s12885-015-1420-9.

Cimpean, Anca-Maria; Ribatti, Domenico; Raica, Marius (2011): A brief history of angiogenesis assays. In *The International journal of developmental biology* 55 (4-5), pp. 377–382. DOI: 10.1387/ijdb.103215ac.

Clarke, Jeffrey Melson; Hurwitz, Herbert I. (2013): Targeted inhibition of VEGF receptor 2: an update on ramucirumab. In *Expert Opin Biol Ther* 13 (8), pp. 1187–1196. DOI: 10.1517/14712598.2013.810717.

Crespin, Sophie; Bechberger, John; Mesnil, Marc; Naus, Christian C.; Sin, Wun-Chey (2010): The carboxy-terminal tail of connexin43 gap junction protein is sufficient to mediate cytoskeleton changes in human glioma cells. In *Journal of cellular biochemistry* 110 (3), pp. 589–597. DOI: 10.1002/jcb.22554.

del Toro, Raquel; Prahst, Claudia; Mathivet, Thomas; Siegfried, Geraldine; Kaminker, Joshua S.; Larrivee, Bruno et al. (2010): Identification and functional analysis of endothelial tip cell-enriched genes. In *Blood* 116 (19), pp. 4025–4033. DOI: 10.1182/blood-2010-02-270819.

Dixelius, Johan; Makinen, Taija; Wirzenius, Maria; Karkkainen, Marika J.; Wernstedt, Christer; Alitalo, Kari; Claesson-Welsh, Lena (2003): Ligand-induced vascular endothelial growth factor receptor-3 (VEGFR-3) heterodimerization with VEGFR-2 in primary lymphatic endothelial cells regulates tyrosine phosphorylation sites. In *The Journal of biological chemistry* 278 (42), pp. 40973–40979. DOI: 10.1074/jbc.M304499200.

Doetschman, T. C.; Eistetter, H.; Katz, M.; Schmidt, W.; Kemler, R. (1985): The in vitro development of blastocyst-derived embryonic stem cell lines: formation of visceral yolk sac, blood islands and myocardium. In *Journal of embryology and experimental morphology* 87, pp. 27–45.

Elling, Ulrich; Penninger, Josef M. (2014): Genome wide functional genetics in haploid cells. In *FEBS letters* 588 (15), pp. 2415–2421. DOI: 10.1016/j.febslet.2014.06.032.

Elling, Ulrich; Taubenschmid, Jasmin; Wirnsberger, Gerald; O'Malley, Ronan; Demers, Simon-Pierre; Vanhaelen, Quentin et al. (2011): Forward and reverse genetics through derivation of haploid mouse embryonic stem cells. In *Cell Stem Cell* 9 (6), pp. 563–574. DOI: 10.1016/j.stem.2011.10.012.

Elling, Ulrich; Wimmer, Reiner A.; Leibbrandt, Andreas; Burkard, Thomas; Michlits, Georg; Leopoldi, Alexandra et al. (2017): A reversible haploid mouse embryonic stem cell biobank resource for functional genomics. In *Nature* 550 (7674), pp. 114–118. DOI: 10.1038/nature24027.

Favier, Benoit; Alam, Antoine; Barron, Pauline; Bonnin, Jacques; Laboudie, Patricia; Fons, Pierre et al. (2006): Neuropilin-2 interacts with VEGFR-2 and VEGFR-3 and promotes human endothelial cell survival and migration. In *Blood* 108 (4), pp. 1243–1250. DOI: 10.1182/blood-2005-11-4447.

Ferrara, N. (1996): Heterozygous embryonic lethality induced by targeted inactivation of the VEGF gene. In *Nature* 380, pp. 439–442.

Folkman, J. (1971): Tumor angiogenesis: therapeutic implications. In *N Engl J Med.* 285 (21), pp. 1182–1186.

Fong, G. H. (1995): Role of the Flt-1 receptor tyrosine kinase in regulating the assembly of vascular endothelium. In *Nature* 376, pp. 66–70.

Fouad, Yousef Ahmed; Aanei, Carmen (2017): Revisiting the hallmarks of cancer. In *American journal of cancer research* 7 (5), pp. 1016–1036.

Gale, Nicholas W.; Dominguez, Melissa G.; Noguera, Irene; Pan, Li; Hughes, Virginia; Valenzuela, David M. et al. (2004): Haploinsufficiency of delta-like 4 ligand results in embryonic lethality due to major defects in arterial and vascular development. In *Proceedings of the National Academy of Sciences of the United States of America* 101 (45), pp. 15949–15954. DOI: 10.1073/pnas.0407290101.

George D. Yancopoulos (2000): Vascular-specific growth factors and blood vessel formation. In *Nature*.

Gerecht-Nir, Sharon; Osenberg, Sivan; Nevo, Ori; Ziskind, Anna; Coleman, Raymond; Itskovitz-Eldor, Joseph (2004): Vascular development in early human embryos and in teratomas derived from human embryonic stem cells. In *Biology of reproduction* 71 (6), pp. 2029–2036. DOI: 10.1095/biolreprod.104.031930.

Gerhardt, H1 (2004): Neuropilin-1 is required for endothelial tip cell guidance in the developing central nervous system. In *Dev Dynam* 231 (3), pp. 503–509.

Geudens, Ilse; Gerhardt, Holger (2011): Coordinating cell behaviour during blood vessel formation. In *Development (Cambridge, England)* 138 (21), pp. 4569–4583. DOI: 10.1242/dev.062323.

Gilbert, Mark R.; Dignam, James J.; Armstrong, Terri S.; Wefel, Jeffrey S.; Blumenthal, Deborah T.; Vogelbaum, Michael A. et al. (2014): A randomized trial of bevacizumab for newly diagnosed glioblastoma. In *N. Engl. J. Med.* 370 (8), pp. 699–708. DOI: 10.1056/NEJMoa1308573.

Goding, James W.; Grobben, Bert; Slegers, Herman (2003): Physiological and pathophysiological functions of the ecto-nucleotide pyrophosphatase/phosphodiesterase family. In *Biochimica et Biophysica Acta (BBA) - Molecular Basis of Disease* 1638 (1), pp. 1–19. DOI: 10.1016/S0925-4439(03)00058-9.

Goggins, Bridie J.; Chaney, Ciaran; Radford-Smith, Graham L.; Horvat, Jay C.; Keely, Simon (2013): Hypoxia and Integrin-Mediated Epithelial Restitution during Mucosal Inflammation. In *Frontiers in immunology* 4, p. 272. DOI: 10.3389/fimmu.2013.00272.

Goldie, Lauren C.; Nix, Melissa K.; Hirschi, Karen K. (2008): Embryonic vasculogenesis and hematopoietic specification. In *Organogenesis* 4 (4), pp. 257–263.

Griffioen, Arjan W.; Thijssen, Victor L. (2014): Galectins in tumor angiogenesis. In *Ann Transl Med* 2 (9), p. 90. DOI: 10.3978/j.issn.2305-5839.2014.09.01.

Haller, B. K.; Bråve, A.; Wallgard, E.; Roswall, P.; Sunkari, V. G.; Mattson, U. et al. (2010): Therapeutic efficacy of a DNA vaccine targeting the endothelial tip cell antigen delta-like

ligand 4 in mammary carcinoma. In *Oncogene* 29 (30), pp. 4276–4286. DOI: 10.1038/onc.2010.176.

Harrington, LS1; Sainson, R. C.; Williams, C. K.; Taylor, J. M.; Shi, W.; Li, J. L.; Harris, AL. (2008): Regulation of multiple angiogenic pathways by Dll4 and Notch in human umbilical vein endothelial cells. In *Microvasc Res 2008* 75 (2), pp. 144–154.

Hartwell, Leland H.; Mortimer, Robert K.; Culotti, Joseph; Culotti, Marilyn (1973): Genetic Control of the Cell Division Cycle in Yeast: V. Genetic Analysis of cdc Mutants. In *Genetics* 74 (2), pp. 267–286.

Hayashi, Makoto; Majumdar, Arindam; Li, Xiujuan; Adler, Jeremy; Sun, Zuyue; Vertuani, Simona et al. (2013): VE-PTP regulates VEGFR2 activity in stalk cells to establish endothelial cell polarity and lumen formation. In *Nat Commun* 4, p. 1672. DOI: 10.1038/ncomms2683.

Hellström M1 (2007): Dll4 signalling through Notch1 regulates formation of tip cells during angiogenesis. In *Nature* 445 (7129), pp. 776–780.

Holderfield, Matthew T.; Henderson Anderson, April M.; Kokubo, Hiroki; Chin, Michael T.; Johnson, Randy L.; Hughes, Christopher C. W. (2006): HESR1/CHF2 suppresses VEGFR2 transcription independent of binding to E-boxes. In *Biochemical and biophysical research communications* 346 (3), pp. 637–648. DOI: 10.1016/j.bbrc.2006.05.177.

Homkajorn, B.; Sims, N. R.; Muyderman, H. (2010): Connexin 43 regulates astrocytic migration and proliferation in response to injury. In *Neuroscience letters* 486 (3), pp. 197–201. DOI: 10.1016/j.neulet.2010.09.051.

Hrabe de Angelis, M.; McIntyre, J. 2nd; Gossler, A. (1997): Maintenance of somite borders in mice requires the Delta homologue DII1. In *Nature* 386 (6626), pp. 717–721. DOI: 10.1038/386717a0.

Jaffe, E. A.; Nachman, R. L.; Becker, C. G.; Minick, C. R. (1973): Culture of human endothelial cells derived from umbilical veins. Identification by morphologic and immunologic criteria. In *J Clin Invest.*

Jakobsson, Lars; Bentley, Katie; Gerhardt, Holger (2009): VEGFRs and Notch: a dynamic collaboration in vascular patterning. In *Biochem. Soc. Trans.* 37 (Pt 6), pp. 1233–1236. DOI: 10.1042/BST0371233.

Jakobsson, Lars; Franco, Claudio A.; Bentley, Katie; Collins, Russell T.; Ponsioen, Bas; Aspalter, Irene M. et al. (2010): Endothelial cells dynamically compete for the tip cell position during angiogenic sprouting. In *Nat. Cell Biol.* 12 (10), pp. 943–953. DOI: 10.1038/ncb2103.

Jakobsson, Lars; Kreuger, Johan; Claesson-Welsh, Lena (2007): Building blood vessels--stem cell models in vascular biology. In *The Journal of cell biology* 177 (5), pp. 751–755. DOI: 10.1083/jcb.200701146.

Jia, Xuelian; Wang, Wenyi; Xu, Zhuobin; Wang, Shijing; Wang, Tong; Wang, Min; Wu, Min (2016): A humanized anti-DLL4 antibody promotes dysfunctional angiogenesis and inhibits breast tumor growth. In *Scientific reports* 6, p. 27985. DOI: 10.1038/srep27985.

Kameritsch, Petra; Pogoda, Kristin; Pohl, Ulrich (2012): Channel-independent influence of connexin 43 on cell migration. In *Biochimica et biophysica acta* 1818 (8), pp. 1993–2001. DOI: 10.1016/j.bbamem.2011.11.016.

Kaur, Gurvinder; Dufour, Jannette M. (2012): Cell lines. Valuable tools or useless artifacts. In *Spermatogenesis* 2 (1), pp. 1–5. DOI: 10.4161/spmg.19885.

Kim, Da; Kim, Yoon; Lee, Hai; Moon, Shin; Ku, Seung-Yup; Kim, Moon (2013): In Vivo Osteogenic Differentiation of Human Embryoid Bodies in an Injectable in Situ-Forming Hydrogel. In *Materials* 6 (7), pp. 2978–2988. DOI: 10.3390/ma6072978.

Koch, Sina; Tugues, Sònia; Li, Xiujuan; Gualandi, Laura; Claesson-Welsh, Lena (2011): Signal transduction by vascular endothelial growth factor receptors. In *Biochem. J.* 437 (2), pp. 169–183. DOI: 10.1042/BJ20110301.

Korekane, Hiroaki; Park, Jong Yi; Matsumoto, Akio; Nakajima, Kazuki; Takamatsu, Shinji; Ohtsubo, Kazuaki et al. (2013): Identification of ectonucleotide pyrophosphatase/phosphodiesterase 3 (ENPP3) as a regulator of N-acetylglucosaminyltransferase GnT-IX (GnT-Vb). In *The Journal of biological chemistry* 288 (39), pp. 27912–27926. DOI: 10.1074/jbc.M113.474304.

Leeb, Martin; Wutz, Anton (2011): Derivation of haploid embryonic stem cells from mouse embryos. In *Nature* 479 (7371), pp. 131–134. DOI: 10.1038/nature10448.

Li, JL1; Sainson, R. C.; Shi, W.; Leek, R.; Harrington, L. S.; Preusser, M. et al. (2007): Delta-like 4 Notch ligand regulates tumor angiogenesis, improves tumor vascular function, and promotes tumor growth in vivo. In *Cancer Res.* 67 (23), pp. 11244–11253.

Li, Zhe; Huang, Hui; Boland, Patricia; Dominguez, Melissa G.; Burfeind, Patricia; Lai, Ka-Man et al. (2009): Embryonic stem cell tumor model reveals role of vascular endothelial receptor tyrosine phosphatase in regulating Tie2 pathway in tumor angiogenesis. In *Proceedings of the National Academy of Sciences of the United States of America* 106 (52), pp. 22399–22404. DOI: 10.1073/pnas.0911189106.

Liao, Y.; Day, K. H.; Damon, D. N.; Duling, B. R. (2001): Endothelial cell-specific knockout of connexin 43 causes hypotension and bradycardia in mice. In *Proceedings of the National Academy of Sciences of the United States of America* 98 (17), pp. 9989–9994. DOI: 10.1073/pnas.171305298.

Lupo, G.; Caporarello, N.; Olivieri, M.; Cristaldi, M.; Motta, C.; Bramanti, V. et al. (2016): Anti-angiogenic Therapy in Cancer: Downsides and New Pivots for Precision Medicine. In *Frontiers in pharmacology* 7, p. 519. DOI: 10.3389/fphar.2016.00519.

Mailhos, C1; Modlich, U.; Lewis, J.; Harris, A.; Bicknell, R.; Ish-Horowicz, D. (2001): Delta4, an endothelial specific notch ligand expressed at sites of physiological and tumor angiogenesis. In *Differentiation* 69, pp. 135–144.

Majumder, Syamantak; Zhu, GuoFu; Xu, Xiangbin; Senchanthisai, Sharon; Jiang, Dongyang; Liu, Hao et al. (2016): G-Protein-Coupled Receptor-2-Interacting Protein-1 Controls Stalk Cell Fate by Inhibiting Delta-like 4-Notch1 Signaling. In *Cell reports* 17 (10), pp. 2532–2541. DOI: 10.1016/j.celrep.2016.11.017.

Maqsood, Muhammad Irfan; Matin, Maryam M.; Bahrami, Ahmad Reza; Ghasroldasht, Mohammad M. (2013): Immortality of cell lines. Challenges and advantages of establishment. In *Cell biology international* 37 (10), pp. 1038–1045. DOI: 10.1002/cbin.10137.

Melly, Ludovic; Boccardo, Stefano; Eckstein, Friedrich; Banfi, Andrea; Marsano, Anna (2012): Cell and gene therapy approaches for cardiac vascularization. In *Cells* 1 (4), pp. 961–975. DOI: 10.3390/cells1040961.

Michaelis, U. Ruth (2014): Mechanisms of endothelial cell migration. In *Cellular and molecular life sciences : CMLS* 71 (21), pp. 4131–4148. DOI: 10.1007/s00018-014-1678-0.

Miele, Lucio (2011): Transcription factor RBPJ/CSL: a genome-wide look at transcriptional regulation. In *Proceedings of the National Academy of Sciences of the United States of America* 108 (36), pp. 14715–14716. DOI: 10.1073/pnas.1110570108.

Mumm, J. S.; Kopan, R. (2000): Notch signalling: from the outside in. In *Developmental biology* 228 (2), pp. 151–165. DOI: 10.1006/dbio.2000.9960.

Nagy, A. (2000): Cre recombinase: the universal reagent for genome tailoring. In *Genesis* 26 (2), pp. 99–109.

Nagy, A.; Vintersten, K. (2006): Murine embryonic stem cells. In *Methods in enzymology* 418, pp. 3–21. DOI: 10.1016/S0076-6879(06)18001-5.

Nakahara, Susumu; Saito, Takashi; Kondo, Nami; Moriwaki, Kenta; Noda, Katsuhisa; Ihara, Shinji et al. (2006): A secreted type of beta1,6 N-acetylglucosaminyltransferase V (GnT-V), a novel angiogenesis inducer, is regulated by gamma-secretase. In *FASEB journal : official publication of the Federation of American Societies for Experimental Biology* 20 (14), pp. 2451–2459. DOI: 10.1096/fj.05-5066com.

Nakayama, Masanori; Nakayama, Akiko; van Lessen, Max; Yamamoto, Hiroyuki; Hoffmann, Sarah; Drexler, Hannes C. A. et al. (2013): Spatial regulation of VEGF receptor endocytosis in angiogenesis. In *Nat. Cell Biol.* 15 (3), pp. 249–260. DOI: 10.1038/ncb2679.

Nilsson, Ingrid; Bahram, Fuad; Li, Xiujuan; Gualandi, Laura; Koch, Sina; Jarvius, Malin et al. (2010): VEGF receptor 2/-3 heterodimers detected in situ by proximity ligation on angiogenic sprouts. In *EMBO J.* 29 (8), pp. 1377–1388. DOI: 10.1038/emboj.2010.30.

Norton, Kerri-Ann; Popel, Aleksander S. (2016): Effects of endothelial cell proliferation and migration rates in a computational model of sprouting angiogenesis. In *Scientific reports* 6, p. 36992. DOI: 10.1038/srep36992.

Olsson, AK1; Dimberg, A.; Kreuger, J.; Claesson-Welsh, L. (2006): VEGF receptor signalling - in control of vascular function. In *Nat Rev Mol Cell Biol.* 7 (5), pp. 359–371.

Park, Kyung Min; Gerecht, Sharon (2014): Harnessing developmental processes for vascular engineering and regeneration. In *Development* 141 (14), pp. 2760–2769. DOI: 10.1242/dev.102194.

Patel, NS1; Li, J. L.; Generali, D.; Poulsom, R.; Cranston, D. W.; Harris, AL. (2005): Up-regulation of delta-like 4 ligand in human tumor vasculature and the role of basal expression in endothelial cell function. In *Cancer Res.* 65 (19), pp. 8690–8697.

Patel-Hett, Sunita; D'Amore, Patricia A. (2011): Signal transduction in vasculogenesis and developmental angiogenesis. In *The International journal of developmental biology* 55 (4-5), pp. 353–363. DOI: 10.1387/ijdb.103213sp.

Pfeifer, Alexander; Ikawa, Masahito; Dayn, Yelena; Verma, Inder M. (2002): Transgenesis by lentiviral vectors. Lack of gene silencing in mammalian embryonic stem cells and preimplantation embryos. In *Proceedings of the National Academy of Sciences of the United States of America* 99 (4), pp. 2140–2145. DOI: 10.1073/pnas.251682798.

Potente, Michael; Gerhardt, Holger; Carmeliet, Peter (2011): Basic and therapeutic aspects of angiogenesis. In *Cell* 146 (6), pp. 873–887. DOI: 10.1016/j.cell.2011.08.039.

Reaume, A. G.; Sousa, P. A. de; Kulkarni, S.; Langille, B. L.; Zhu, D.; Davies, T. C. et al. (1995): Cardiac malformation in neonatal mice lacking connexin43. In *Science (New York, N.Y.)* 267 (5205), pp. 1831–1834.

Risau, W. (1997): Mechanisms of angiogenesis. In *Nature* 386 (6626), pp. 671–674. DOI: 10.1038/386671a0.

Rival-Gervier, Sylvie; Lo, Mandy Ym; Khattak, Shahryar; Pasceri, Peter; Lorincz, Matthew C.; Ellis, James (2013): Kinetics and epigenetics of retroviral silencing in mouse embryonic stem cells defined by deletion of the D4Z4 element. In *Molecular therapy : the journal of the American Society of Gene Therapy* 21 (8), pp. 1536–1550. DOI: 10.1038/mt.2013.131.

Rundhaug, Joyce E. (2005): Matrix metalloproteinases and angiogenesis. In *Journal of cellular and molecular medicine* 9 (2), pp. 267–285.

Saito, Takashi; Miyoshi, Eiji; Sasai, Ken; Nakano, Norihiko; Eguchi, Hironobu; Honke, Koich; Taniguchi, Naoyuki (2002): A secreted type of beta 1,6-N-acetylglucosaminyltransferase V (GnT-V) induces tumor angiogenesis without mediation of glycosylation: a novel function of GnT-V distinct from the original glycosyltransferase activity. In *The Journal of biological chemistry* 277 (19), pp. 17002–17008. DOI: 10.1074/jbc.M200521200.

Sakurai Y1 (2005): Essential role of Flk-1 (VEGF receptor 2) tyrosine residue 1173 in vasculogenesis in mice. In *Proc Natl Acad Sci U S A* 102 (4), pp. 1076–1081.

Sawamiphak, Suphansa; Seidel, Sascha; Essmann, Clara L.; Wilkinson, George A.; Pitulescu, Mara E.; Acker, Till; Acker-Palmer, Amparo (2010): Ephrin-B2 regulates VEGFR2 function in developmental and tumor angiogenesis. In *Nature* 465 (7297), pp. 487–491. DOI: 10.1038/nature08995.

Schnütgen, Frank; De-Zolt, Silke; van Sloun, Petra; Hollatz, Melanie; Floss, Thomas; Hansen, Jens et al. (2005): Genomewide production of multipurpose alleles for the functional analysis of the mouse genome. In *Proc. Natl. Acad. Sci. U.S.A.* 102 (20), pp. 7221–7226. DOI: 10.1073/pnas.0502273102.

Schnütgen, Frank; Hansen, Jens; De-Zolt, Silke; Horn, Carsten; Lutz, Marcus; Floss, Thomas et al. (2008): Enhanced gene trapping in mouse embryonic stem cells. In *Nucleic Acids Res.* 36 (20), pp. e133. DOI: 10.1093/nar/gkn603.

Semprini, S.; Troup, T. J.; Kotelevtseva, N.; King, K.; Davis, J. R. E.; Mullins, L. J. et al. (2007): Cryptic loxP sites in mammalian genomes: genome-wide distribution and relevance for the efficiency of BAC/PAC recombineering techniques. In *Nucleic Acids Res.* 35 (5), pp. 1402–1410. DOI: 10.1093/nar/gkl1108.

Shalaby, F. (1995): Failure of blood-island formation and vasculogenesis in Flk-1-deficient mice. In *Nature* 376 (6535), pp. 62–66.

Siemerink, Martin J.; Klaassen, Ingeborg; Van Noorden, Cornelis J F; Schlingemann, Reinier O. (2013): Endothelial tip cells in ocular angiogenesis: potential target for anti-angiogenesis therapy. In *J. Histochem. Cytochem.* 61 (2), pp. 101–115. DOI: 10.1369/0022155412467635.

Smet, Frederik de; Segura, Inmaculada; Bock, Katrien de; Hohensinner, Philipp J.; Carmeliet, Peter (2009): Mechanisms of vessel branching: filopodia on endothelial tip cells lead the way. In *Arteriosclerosis, thrombosis, and vascular biology* 29 (5), pp. 639–649. DOI: 10.1161/ATVBAHA.109.185165.

Sohl, Goran; Willecke, Klaus (2004): Gap junctions and the connexin protein family. In *Cardiovascular research* 62 (2), pp. 228–232. DOI: 10.1016/j.cardiores.2003.11.013.

Strasser, Geraldine A.; Kaminker, Joshua S.; Tessier-Lavigne, Marc (2010): Microarray analysis of retinal endothelial tip cells identifies CXCR4 as a mediator of tip cell morphology and branching. In *Blood* 115 (24), pp. 5102–5110. DOI: 10.1182/blood-2009-07-230284.

Swift, Matthew R.; Weinstein, Brant M. (2009): Arterial-venous specification during development. In *Circulation research* 104 (5), pp. 576–588. DOI: 10.1161/CIRCRESAHA.108.188805.

Tammela, Tuomas; Zarkada, Georgia; Nurmi, Harri; Jakobsson, Lars; Heinolainen, Krista; Tvorogov, Denis et al. (2011): VEGFR-3 controls tip to stalk conversion at vessel fusion

sites by reinforcing Notch signalling. In *Nat. Cell Biol.* 13 (10), pp. 1202–1213. DOI: 10.1038/ncb2331.

Tammela, Tuomas; Zarkada, Georgia; Wallgard, Elisabet; Murtomaki, Aino; Suchting, Steven; Wirzenius, Maria et al. (2008): Blocking VEGFR-3 suppresses angiogenic sprouting and vascular network formation. In *Nature* 454 (7204), pp. 656–660. DOI: 10.1038/nature07083.

Tung, Jennifer J.; Tattersall, Ian W.; Kitajewski, Jan (2012): Tips, stalks, tubes: notch-mediated cell fate determination and mechanisms of tubulogenesis during angiogenesis. In *Cold Spring Harb Perspect Med* 2 (2), pp. a006601. DOI: 10.1101/cshperspect.a006601.

Ubezio, Benedetta; Blanco, Raquel Agudo; Geudens, Ilse; Stanchi, Fabio; Mathivet, Thomas; Jones, Martin L. et al. (2016): Synchronization of endothelial Dll4-Notch dynamics switch blood vessels from branching to expansion. In *eLife* 5. DOI: 10.7554/eLife.12167.

Venkatraman, Lakshmi; Regan, Erzsebet Ravasz; Bentley, Katie (2016): Time to Decide? Dynamical Analysis Predicts Partial Tip/Stalk Patterning States Arise during Angiogenesis. In *PloS one* 11 (11), e0166489. DOI: 10.1371/journal.pone.0166489.

Volinsky, Natalia; Kholodenko, Boris N. (2013): Complexity of receptor tyrosine kinase signal processing. In *Cold Spring Harbor perspectives in biology* 5 (8), a009043. DOI: 10.1101/cshperspect.a009043.

Wang, De-Guo; Zhang, Feng-Xiang; Chen, Ming-Long; Zhu, Hong-Jun; Yang, Bing; Cao, Ke-Jiang (2014): Cx43 in mesenchymal stem cells promotes angiogenesis of the infarcted heart independent of gap junctions. In *Molecular medicine reports* 9 (4), pp. 1095–1102. DOI: 10.3892/mmr.2014.1923.

Wang, Hsueh-Hsiao; Su, Cheng-Huang; Wu, Yih-Jer; Li, Jiun-Yi; Tseng, Ya-Ming; Lin, Yi-Chun et al. (2013): Reduction of connexin43 in human endothelial progenitor cells impairs the angiogenic potential. In *Angiogenesis* 16 (3), pp. 553–560. DOI: 10.1007/s10456-013-9335-z.

Wang, Yingdi; Nakayama, Masanori; Pitulescu, Mara E.; Schmidt, Tim S.; Bochenek, Magdalena L.; Sakakibara, Akira et al. (2010): Ephrin-B2 controls VEGF-induced angiogenesis and lymphangiogenesis. In *Nature* 465 (7297), pp. 483–486. DOI: 10.1038/nature09002.

Wimmer, Reiner; Cseh, Botond; Maier, Barbara; Scherrer, Karina; Baccarini, Manuela (2012): Angiogenic sprouting requires the fine tuning of endothelial cell cohesion by the Raf-1/Rok-α complex. In *Developmental cell* 22 (1), pp. 158–171. DOI: 10.1016/j.devcel.2011.11.012.

Xue, Y.; Gao, X.; Lindsell, C. E.; Norton, C. R.; Chang, B.; Hicks, C. et al. (1999): Embryonic lethality and vascular defects in mice lacking the Notch ligand Jagged1. In *Human molecular genetics* 8 (5), pp. 723–730.

Yancopoulos, GD1; Davis, S.; Gale, N. W.; Rudge, J. S.; Wiegand, S. J.; Holash, J. (2000): Vascular-specific growth factors and blood vessel formation. In *Nature. 2000 Sep 14;407(6801):242-* 407 (6801), pp. 242–248.

Zhang, Luqing; Zhou, Fei; Han, Wencan; Shen, Bin; Luo, Jincai; Shibuya, Masabumi; He, Yulong (2010): VEGFR-3 ligand-binding and kinase activity are required for lymphangiogenesis but not for angiogenesis. In *Cell Res.* 20 (12), pp. 1319–1331. DOI: 10.1038/cr.2010.116.

Zhou, S.; Hayward, S. D. (2001): Nuclear localization of CBF1 is regulated by interactions with the SMRT corepressor complex. In *Molecular and cellular biology* 21 (18), pp. 6222–6232.